

SYNTHESIS TECHNIQUES  
FOR  
BUILT-IN SELF-TESTABLE DESIGNS

LaNae Joy Avra

CRC Technical Report No. 94-6  
(CSL TR 94-633)  
July 1994

CENTER FOR RELIABLE COMPUTING  
Computer Systems Laboratory  
Departments of Electrical Engineering and Computer Science  
Stanford University  
Stanford, CA 94305-4055

Copyright © 1994 by LaNae Joy Avra  
All Rights Reserved

SYNTHESIS TECHNIQUES  
FOR  
BUILT-IN SELF-TESTABLE DESIGNS

A DISSERTATION  
SUBMITTED TO THE DEPARTMENT OF ELECTRICAL ENGINEERING  
AND THE COMMITTEE ON GRADUATE STUDIES  
OF STANFORD UNIVERSITY  
IN PARTIAL FULFILLMENT OF THE REQUIREMENTS  
FOR THE DEGREE OF  
DOCTOR OF PHILOSOPHY

LaNae Joy Avra

June 1994

## ABSTRACT

Hardware synthesis techniques automatically generate a structural hardware implementation given an abstract description of the behavior of the design. Many different hardware designs can implement a given behavioral description, a subset of which also meet specified requirements such as cost, performance, and testability. Existing synthesis techniques typically use minimum cost or maximum performance as the primary criteria for selecting the best hardware implementation. This dissertation describes new synthesis techniques whose primary objective is to satisfy requirements associated with a specific built-in self-test (BIST) architecture.

The use of BIST techniques (design techniques that allow a circuit to test itself) has long been recognized as a means to reduce system life cycle test and maintenance costs. BIST provides shorter test times and allows the use of low-cost test equipment during all stages of the product life: production test, acceptance test, field maintenance, and failure diagnosis. However, hardware overhead, performance degradation, and increased design time are often cited as reasons for the limited use of BIST. When BIST techniques are used, they are often added after the system logic has been designed. At this point, system logic features that may increase BIST overhead or reduce the effectiveness of the BIST operation are expensive to change.

This dissertation describes new synthesis techniques that address two of the major issues associated with BIST: 1) implementation costs due to increased design time, area overhead, increased power consumption, and performance degradation and 2) test effectiveness due to system logic design decisions. Our synthesis procedures use criteria associated with the specified BIST architecture to guide the generation of the system logic, allowing for design decisions that reduce BIST overhead and improve BIST effectiveness. In particular, the primary objective of our synthesis techniques is to generate low-cost, built-in self-testable designs that are free of the types of system bistable dependencies that can reduce the effectiveness of the embedded, multiple input signature registers (MISRs) that are used to perform BIST operations.

One type of system bistable dependency that can be a problem for BIST occurs in a self-adjacent register, where the register inputs are a function of its outputs. To address this problem, we have developed a high-level synthesis technique that minimizes the number of self-adjacent registers in the generated design without increasing the latency of the design. Some system bistable dependencies provide opportunities for sharing BIST and scan logic with system logic, reducing the area and improving the performance of the design. We show that introducing certain, beneficial types of *scan dependence* in the design can increase logic sharing opportunities and can improve BIST effectiveness. Other BIST design techniques attempt to avoid all types of scan dependence. We have developed a logic synthesis technique that analyzes the system bistable dependencies, then arranges the bistables in the MISR to maximize beneficial

scan dependence. For data path logic, we have developed a new scan path architecture, called *orthogonal scan path*, for which the shift direction is orthogonal to the shift direction in traditional scan paths. We show that using an orthogonal scan path increases the number of beneficial scan dependencies between data path logic bistables. We have implemented our synthesis-for-BIST techniques in a computer-aided design system, which serves as a platform for experimentation with existing and future synthesis-for-test techniques.

## ACKNOWLEDGMENTS

I express my deepest appreciation to my adviser, Edward J. McCluskey, for his guidance, support, and instruction during my time at Stanford. His suggestions have greatly enhanced both the technical content and the presentation of this dissertation, and his enthusiasm for learning and for teaching have been a constant source of inspiration.

I am most grateful to my colleagues at the Center for Reliable Computing who have provided many hours of discussions, manuscript editing, and companionship: Piero Franco, Hong Hao, Siyad Ma, Samy Makar, Samiha Mourad, Rob Norwood, Nirmal Saxena, Alice Tokarnia, and Nur Touba. I especially wish to thank the CRC visitors who have worked so diligently on the Odin software: Jean-Charles Giomi, Françoise Martinolle, Laurent Gerbaux, Dave Brokaw, and Gian Luigi Sartori. Their contributions have greatly improved the quality and usefulness of the tool. Many thanks, also, to Siegrid Munda for her expert administrative support.

I would like to thank my associate adviser, Giovanni De Micheli, for his useful comments and suggestions for developing the high-level synthesis algorithms. Thanks, also, to the members of his group that provided support and technical advice: David Ku, Michiel Ligthart, Polly Siegel, and Jerry Yang.

I greatly appreciate the industry feedback and software donations provided by Dave Coelho and Rick Lazansky of Vantage Analysis Systems, Inc., and Jacob El Ziq of Compass Design Automation.

Finally, I wish to thank my family. I thank my husband, Rick, for his support, encouragement, and technical advice. His expertise in the design, validation, testing, and manufacturing of VLSI chips provided invaluable real-world perspective to the material in this dissertation. I am grateful to both Rick and my daughter, Tamsin, for their patience, understanding, and unconditional love, without which this work would not have been possible. Thanks, also, to my parents for instilling in me the self-confidence necessary to pursue my goals and for providing me with every opportunity to learn.

This work was supported in part by Digital Equipment Corporation, Low-End Diagnostics Group, and in part by the Innovative Science and Technology Office of the Strategic Defense Initiative Organization and administered through the Office of Naval Research under Contract Nos. N00014-85-K-0600 and N00014-92-J-1782, and in part by the National Science Foundation under grant Nos. MIP-8709128 and MIP-9107760.

# TABLE OF CONTENTS

Abstract .....	i
Acknowledgments.....	iii
List of Tables .....	vi
List of Illustrations .....	vii
<b>1 Introduction.....</b>	<b>1</b>
1.1 Motivation .....	1
1.2 Contributions.....	3
1.3 Outline.....	4
<b>2 Embedded BIST Architectures .....</b>	<b>5</b>
2.1 Parallel BIST Architecture .....	6
2.2 Circular BIST Architecture .....	12
2.3 Reconfigurable Register Design .....	13
<b>3 Allocation and Binding for Parallel BIST.....</b>	<b>16</b>
3.1 High-Level Synthesis Tasks.....	17
3.2 Register Conflict Graph .....	18
3.3 Implementation and Results .....	20
3.4 Contributions.....	22
<b>4 Synthesis for Scan Dependence.....</b>	<b>24</b>
4.1 Scan Dependence .....	25
4.2 Synthesis for Scan Dependence .....	28
4.3 Implementation and Results .....	30
4.3.1 Area and Delay Results.....	31
4.3.2 Fault Simulation Results .....	34
4.4 Contributions.....	35
<b>5 Scan Dependence in Data Path Logic .....</b>	<b>36</b>
5.1 Orthogonal Scan Path Architecture.....	37
5.2 Scan Dependence Functions in Data Path Logic .....	37
5.3 Results .....	39
5.4 Contributions.....	40
<b>6 Synthesis-for-Test Design System.....</b>	<b>41</b>

6.1	Overview .....	41
6.2	Design System Input and Output .....	42
6.2.1	VHDL Descriptions .....	43
6.2.2	Component Library .....	44
6.3	Data and Control Flow Graphs .....	44
6.4	High-Level Synthesis Techniques .....	47
7	Concluding Remarks .....	50
	References .....	52

## LIST OF TABLES

Table 2-1	Test session register configurations for design example in [Hudson 87].	8
Table 3-1	Register binding algorithm for parallel BIST register conflict graph.	21
Table 3-2	Comparison of synthesis procedures on Tseng [Tseng 86] and DiffEq [Paulin 89a] data flow descriptions.	22
Table 4-1	Area and delay for shaded logic in Fig. 4-3 based on data in [LSI 91].	28
Table 4-2	Scan dependence classification of decomposed Boolean equations.	29
Table 4-3	Bistable characteristics for circular BIST benchmark circuits.	32
Table 4-4	Area and overhead for area-optimized circular BIST benchmark circuits.	32
Table 4-5	Delay and overhead for delay-optimized circular BIST benchmark circuits.	33
Table 4-6	Layout area overhead for area-optimized circular BIST benchmark circuits.	33
Table 4-7	Fault simulation results for circular BIST benchmark circuits.	35
Table 5-1	System equations for data path registers that benefit from scan dependence.	38
Table 5-2	Data path design examples with orthogonal scan path and circular BIST.	40
Table 6-1	Example VHDL behavioral description	43
Table 6-2	Example VHDL structural description of data path logic generated by Odin.	44

## LIST OF ILLUSTRATIONS

Figure 1-1	Test scenario for life cycle of integrated circuit part. ....	1
Figure 1-2	Built-in self-test configuration. ....	2
Figure 2-1	Parallel BIST architecture. ....	7
Figure 2-2	Self-adjacent register implemented with CBILBO. ....	9
Figure 2-3	LFSR and MISR configurations for Fig. 2-1. ....	11
Figure 2-4	Circular BIST architecture. ....	13
Figure 2-5	Reconfigurable register. ....	14
Figure 2-6	MISR error capture capabilities. ....	15
Figure 3-1	High-level synthesis example. ....	17
Figure 3-2	Register conflict graph example. ....	19
Figure 3-3	Testability conflict edges. ....	20
Figure 4-1	Embedded MISR with scan dependence. ....	25
Figure 4-2	Fault simulation results of BIST operation of circular BIST circuits with maximum scan dependence. ....	26
Figure 4-3	Scan dependence solutions for $Z2 = Q1 + f$ . ....	28
Figure 4-4	Beneficial scan dependence implementations. ....	29
Figure 5-1	Orthogonal scan path example. ....	37
Figure 5-2	Live variable motion. ....	40
Figure 6-1	Odin design system overview. ....	42
Figure 6-2	DCFG example. ....	45
Figure 6-3	Data flow graphs. ....	46
Figure 6-4	High-level synthesis example. ....	48
Figure 6-5	Control logic state machine description for Fig. 6-2. ....	49



# 1 INTRODUCTION

## 1.1 MOTIVATION

An integrated circuit part such as a chip, multi-chip module, board, or system must be thoroughly tested in order to determine whether or not it is defective. Different types of tests are applied to the part at various times in its life cycle to detect different types of failures. For example, the part manufacturer applies production tests to the part to determine whether or not there are manufacturing defects, whereas the end user applies field tests to identify failures caused by stressful conditions in the operating environment (e.g., radiation, vibration) or reliability problems within the part (e.g., electromigration). Figure 1-1 illustrates a possible test scenario that encompasses the entire life cycle of an integrated circuit part. In the first phase of testing, the manufacturer applies production tests in order to prevent parts with manufacturing defects from being shipped to the customer. Next, the customer applies acceptance tests to determine whether or not the parts should be placed in field operation. Acceptance tests identify parts that have been damaged during shipping, or parts that don't meet customer specifications. Parts that pass acceptance testing are then assembled into systems and placed into field operation. Field tests are applied to a system that has failed in the field in order to identify the defective component parts that must be replaced. For each testing phase in this particular scenario, diagnostic tests are applied to rejected parts to determine the cause of failure in an effort to improve the manufacturing process.

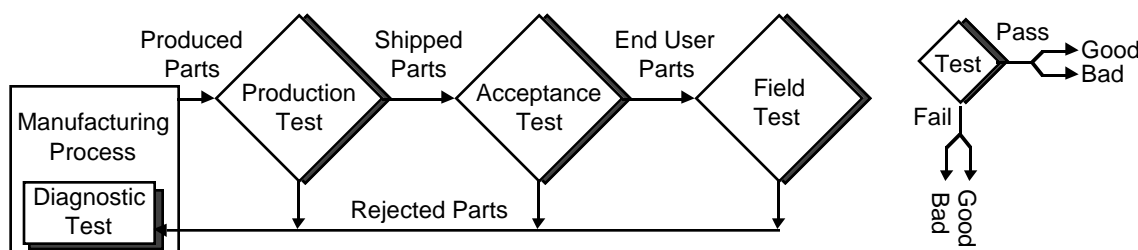


**Figure 1-1** Test scenario for life cycle of integrated circuit part.

The goal in any test scenario is to apply the most rigorous tests possible, tests for which the number of good parts that fail, but most importantly, the number of bad parts that pass (called *test escapes*) are minimized. The quality of a test is a function of how many of the targeted failures are detected by the test, how well the targeted failures represent actual defects, and how easily the part can be tested. As integrated circuit parts become more and more complex, dense, and inaccessible, rigorous testing becomes less feasible unless design practices are used that allow for easier testing. These design practices, called *design-for-testability (DFT)* techniques, simplify the test development task by constraining the design to easy-to-test structures, thereby making it easier to generate and apply tests that detect all of the targeted failures. However,

rigorous testing can still be impractical due to the expensive external test equipment required to apply the tests.

Built-in self-test (BIST) is a DFT technique that allows a part to test itself. BIST techniques such as those described in [McCluskey 85], [McCluskey 86], [Bardell 87], and [Abramovici 90] have long been recognized as a means to reduce life cycle test and maintenance costs by embedding external tester features, such as *test pattern generation (TPG)* and *output response analysis (ORA)*, into the part that contains the *circuit under test (CUT)* (Fig. 1-2). BIST can provide shorter test times than externally-applied tests and allows the use of low-cost test equipment during all stages of the product life including system debug, production test, field maintenance, and failure diagnosis. Even though industry use of BIST techniques is becoming more common [Gelsinger 86], [Lake 86], [Nozuyama 88], [Ratiu 90], [Starke 90], [Bardell 91], [Illman 91], [Preissner 92], [Sinaki 92], [Yokomizo 92], [Bonnenberg 93], [Broseghini 93], [Gage 93], [Langford 93], [Patel 93], area overhead, performance degradation, and increased design time are often cited as reasons for the limited use of BIST.

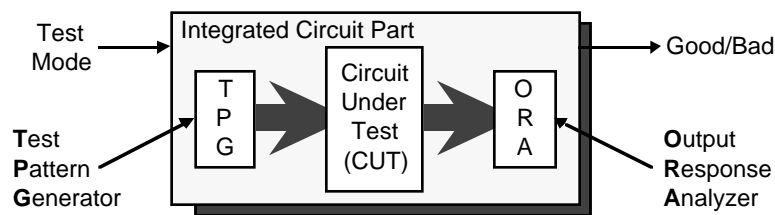


**Figure 1-2** Built-in self-test configuration.

Traditional design methods separate the tasks of system logic design (design of the logic that implements the normal operation of the part) and BIST logic design. During the initial stages of design, system logic issues take priority over BIST issues such as selection of the most appropriate BIST technique for the system logic, BIST logic implementation, and evaluation of the BIST operation. As the design progresses, time-to-market pressures often cause the postponement of BIST design until the end of the design process at which point little time is available to address BIST issues, and any mistakes made are expensive to fix. Automated *BIST synthesis* techniques, where BIST logic is added or a BIST architecture is selected after the system logic has been designed [Abadir 85], [Zhu 88], are valuable in that they reduce the design time and the number of design mistakes by automating the BIST logic design process. Unfortunately, earlier system logic design decisions can reduce the effectiveness and increase the overhead of the implemented BIST technique.

Hardware synthesis techniques automatically generate a structural hardware implementation given an abstract description of the behavior of the part. Many different hardware designs can implement a given behavioral description, a subset of which also meet specified requirements such as cost, performance, and testability. Current research in hardware synthesis techniques

(e.g., [Brayton 87], [McFarland 88], [De Micheli 94]) typically focuses on the use of minimum area or maximum performance as the primary criteria for selecting the best hardware implementation. Some *synthesis-for-testability* techniques attempt to generate the lowest-cost, highest-performance implementation that also meets certain specified testability requirements such as irredundant combinational logic [Hachtel 89], [Bryan 89] or robustly delay-fault testable logic [Devadas 90], [Jha 92]. Testable logic is a necessary, but not sufficient, condition for high-quality BIST operation. This dissertation describes new *synthesis-for-BIST* techniques that have the primary objective of satisfying requirements associated with a specific BIST architecture when generating the system logic structural implementation. Cost is minimized and performance is maximized to the extent that BIST requirements are not compromised. These new synthesis techniques address two of the major issues associated with generating self-testable designs: 1) increased implementation costs due to added design time, area overhead, and performance degradation, and 2) reduced self-test effectiveness due to system logic design decisions. Considering BIST issues during system logic synthesis allows for the generation of system logic that is optimized for a particular BIST architecture and that can be more effectively tested by the BIST operation.

## 1.2 CONTRIBUTIONS

This dissertation describes new synthesis techniques that use the requirements of the implemented BIST architecture to guide the synthesis of the system logic in order to improve the effectiveness of the self-test operation and to reduce the BIST logic overhead. In developing these new techniques, we have focused on embedded BIST architectures because they provide opportunities for the sharing of system and test logic. Logic sharing makes it possible to reduce the area overhead of the BIST logic and improve the performance of the generated design. In particular, the following are the contributions of this dissertation:

- We have developed and implemented a *new register allocation and binding algorithm* for high-level synthesis that generates designs with a minimum number of self-adjacent registers [Avra 91]. This technique is used for parallel BIST architectures.
- We have formalized the concept of *scan dependence* in embedded BIST architectures and have presented fault simulation data showing that, if ignored, scan dependence can significantly reduce the effectiveness of the BIST operation [Avra 94a].
- We have identified certain types of scan dependence that can be beneficial to the design and have developed *new output response analysis (ORA) structures* that take advantage of them [Avra 93], [Avra 94a].
- We have developed and implemented a *new synthesis for scan dependence technique* that maximizes the amount of beneficial scan dependence in the design [Avra 93], [Avra 94a].

- We have developed a *new scan path architecture* that increases the amount of beneficial scan dependence in data path logic [Avra 92].
- We have implemented a *synthesis-for-test computer-aided design tool* that includes the synthesis techniques described in this dissertation and generates a self-testable design given a behavioral VHDL description of the design [Avra 90], [Avra 94b].

### **1.3 OUTLINE**

This dissertation is organized as follows. In Sec. 2, we describe in detail the operation and implementation of two embedded BIST architectures: parallel BIST and circular BIST. Parallel BIST is the target BIST architecture of the synthesis technique described in Sec. 3, and circular BIST is the target architecture of the synthesis techniques described in Secs. 4 and 5. We also describe a register design that can be used in the parallel and circular BIST architectures. We use this register design to illustrate the BIST concepts and design techniques presented in the remainder of the dissertation. In general, each section discussing the contributions of this dissertation (Secs. 3-6) is a summary of material previously published by the author and included in Appendices I-IV. Section 3 contains a description of a high-level synthesis technique that generates the system logic for a parallel BIST architecture. In Sec. 4, we define scan dependence and illustrate its advantages and disadvantages with a simple example. We then describe a synthesis technique that arranges the system bistables into MISRs such that beneficial scan dependence is maximized. We illustrate the technique using the circular BIST architecture. In Sec. 5, we show that beneficial scan dependence can be increased in data path logic when an orthogonal scan path configuration is used. Section 6 is an overview of the synthesis-for-test computer-aided design tool the implements the described synthesis techniques. The tool is intended to be a platform for experimentation with existing and future test synthesis and synthesis-for-test techniques. Section 7 concludes this dissertation.

## 2 EMBEDDED BIST ARCHITECTURES

BIST techniques are implemented by including a *test pattern generator (TPG)* and *output response analyzer (ORA)* in the part (e.g., chip, multi-chip module, board) that contains the *circuit under test (CUT)*. During BIST operation, the TPG applies test patterns to the inputs of the CUT and the ORA captures the response of the CUT to those test patterns. Typically, the TPG and ORA are implemented such that they automatically generate patterns and analyze responses at test time so that the test pattern and test response storage requirements are minimized. *Embedded* BIST architectures use reconfigurable system bistables to implement both the normal system operation and the BIST TPG and ORA operations. Since the BIST logic is combined with the system logic, opportunities exist for synthesis technique to generate hardware that can be shared by both the system and test operations, resulting in improved performance and reduced cost. However, in addition to system logic issues such as performance and cost, the synthesis technique must be capable of addressing issues that affect the quality of the BIST operation, issues such as self-test time, and TPG and ORA effectiveness. We discuss these issues in this section.

Most BIST architectures use pseudo-random pattern generators such as *linear feedback shift registers (LFSRs)* or weighted random pattern generators [Waicukauski 89] to perform TPG operations. The TPGs are called *pseudo-random* because, while they generate patterns with characteristics that are similar to randomly-generated patterns, their behavior is deterministic. The test is therefore repeatable, and the results of the test can be compared with expected results. In order to test for all possible combinational faults (e.g., single and multiple stuck-at faults) within an  $n$ -input cone of combinational logic in the CUT, where a cone of logic is delimited by starting at a combinational logic output (either a primary output or a bistable input) and tracing backwards through the gates to each input (either a primary input or a bistable output), a TPG must be capable of applying all  $2^n$  possible test patterns. To test for pattern-dependent faults [Hao 91], delay faults, or faults that cause combinational logic to behave sequentially, the TPG may be required to generate multiple sequences of the  $2^n$  possible patterns. Faults that affect more than one cone of logic (e.g., a bridging fault between the inputs of two logic gates that are in different cones) can be detected if a single TPG covers multiple cones. We evaluate the TPGs generated by our synthesis techniques in terms of their ability to generate  $2^n$  different test patterns for each  $n$ -input cone of logic. Even though it may be determined that not all of the  $2^n$  test patterns need to be applied during BIST operation, it is difficult to determine *a priori* which subset of test patterns will be required to provide a high fault coverage test for each CUT. Therefore, the TPGs must be designed such that they could generate all  $2^n$  different test patterns if necessary. This is known as the “philosophy of possible exhaustion” [Bardell 87]. Also, if all

$2^n$  test patterns can be generated, one can use probabilistic models, based on the number of test patterns applied and the detectabilities of the faults in the CUT, to estimate the fault coverage provided by the TPG [McCluskey 88], thus avoiding expensive and time-consuming fault simulations.

An ideal ORA is capable of analyzing the response of each test pattern applied to the CUT. In practice, of course, this is not feasible for a built-in ORA. Instead, most BIST architectures use ORAs, such as *multiple-input signature registers (MISRs)*, that compact the test response, resulting in a loss of information. Thus, under certain error conditions, the test response of a faulty CUT may be indistinguishable from the test response of a fault-free CUT, a phenomenon known as *aliasing*. Our synthesis techniques assume that MISRs are used as the ORAs in the implemented BIST architecture and attempt to minimize the amount of aliasing in those MISRs.

In this section, we describe two embedded BIST architectures, parallel BIST and circular BIST, and discuss BIST-related synthesis issues for each. In Sec. 2.1, we describe parallel BIST, emphasizing often-overlooked implementation complexities that must be addressed by the synthesis technique so that it generates a design that performs a high-quality BIST operation. The synthesis technique described in Sec. 3 generates designs with parallel BIST architectures. The synthesis techniques described in Secs. 4 and 5, though applicable to all BIST architectures that use embedded MISRs, generate designs that use the circular BIST technique. We describe the assumed circular BIST architecture in Sec. 2.2. In Sec. 2.3, we describe one possible implementation of a reconfigurable register design for embedded BIST architectures. The register is configured as a normal parallel load register for system operation. During BIST operation, it is configured as either a maximum-length LFSR for test pattern generation or as a MISR for output response analysis.

## **2.1 PARALLEL BIST ARCHITECTURE**

The parallel BIST architecture [Konemann 80] is an embedded BIST architecture in which system registers are reconfigured to perform either LFSR or MISR operations during BIST. The *built-in logic block observer (BILBO)* register [Konemann 79] is often used to implement the system registers in parallel BIST architectures. A possible implementation of the BILBO register is described in detail in Sec. 2.3. Variations of the parallel BIST architecture are discussed in [McCluskey 81], [Krasniewski 85], [Hudson 87].

Figure 2-1 illustrates how the parallel BIST architecture is used to test a block of data path logic that consists of five registers (*R1-R5*), five combinational logic units (*CLU1-CLU5*), primary input signals (*PI*), and primary output signals (*PO*). During normal operation (Fig. 2-1a), the system registers are configured to load data from the outputs of the CLUs. Prior to performing BIST operation, the system bistables must begin in a known state. This can be

accomplished by configuring the registers into a scan path and shifting in known data or by configuring the registers to perform a reset operation. During BIST operation, the registers are configured as either LFSRs or MISRs. At each clock cycle, pseudo-random test patterns are applied to the inputs of the CLUs by the LFSRs at the same time that the test results (the outputs of the CLUs) are compacted in the MISRs. Figures 2-1b and 2-1c represent two different *test sessions* of the BIST operation, where each test session consists of a unique mapping of registers to LFSRs and MISRs. *CLU3*, *CLU4*, and *CLU5* are tested during the first test session (Fig. 2-1b), and *CLU1* and *CLU2* are tested during the second test session (Fig. 2-1c). After each test session, the registers are configured into a serial shift path so that the test results can be shifted out and compared with expected results. This comparison can be performed either by external test equipment or by BIST control logic that may be included as part of a test access port controller [IEEE 90]. The BIST control logic also generates signals that control the configuration of the system registers.

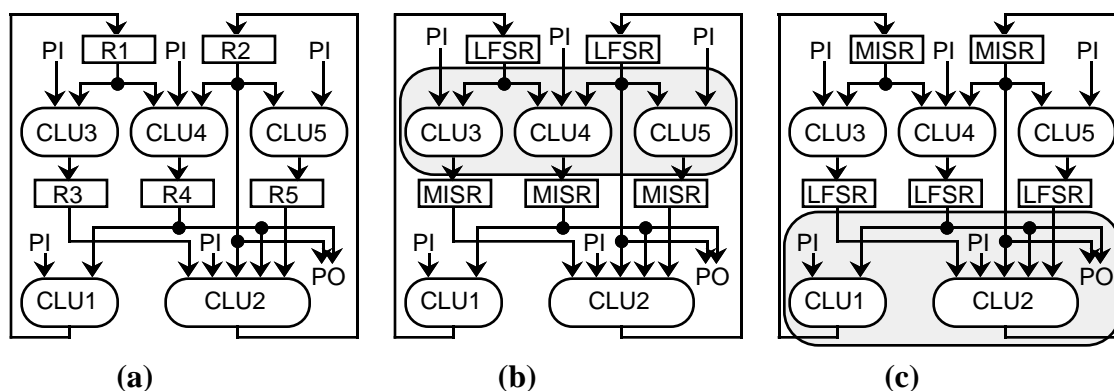


**Figure 2-1** Parallel BIST architecture: (a) normal operation; (b) first test session configuration; (c) second test session configuration.

One advantage of the parallel BIST architecture is that it supports *at-speed self-test operation*: a new test pattern is applied to the CUT at each clock cycle. At-speed operation means that the parallel BIST technique may be able to detect some delay faults. Another advantage of this technique is that, since each system register can be reconfigured as either an LFSR or a MISR, multiple CLUs can be tested in parallel, reducing the total self-test time.

We define an ideal parallel BIST architecture as one for which the system bistables can be arranged into LFSRs and MISRs such that, for each  $n$ -input CLU in the design,  $2^n$  different test patterns can be applied to the CLU inputs during the same test session that the CLU outputs are captured in a MISR. Unfortunately, due to the inter-connectedness of the system bistables in typical designs, many test sessions may be required to test all of the CLUs in an ideal parallel BIST architecture. For example, register interconnection data and test session configurations for a twenty-three register, parallel BIST design is provided in [Hudson 87]. This information is

shown in a different form in Table 2-1, which lists which registers, numbered 1 through 23, are configured as LFSRs and MISRs for each test session. We assume that any CLU feeding a register that is configured as a MISR during a given test session is tested during that test session. For example, during test session 10, the CLUs that feed registers 9 and 16 are tested by test patterns supplied by registers 10, 12, and 17. Registers 9, 16, 10, and 12 in Table 2-1 could be interconnected in the same manner as registers *R4*, *R3*, *R1*, and *R2*, respectively, in Fig. 2-1a. The design requires a minimum of twelve different test sessions, where an average of 1.75 registers are configured as MISRs and 13.9 registers are configured as LFSRs in each test session. The high number of test sessions corresponds to the low degree of self-test parallelism in the design.

**Table 2-1** Test session register configurations for design example in [Hudson 87].

Test Session	MISRs	LFSRs
1	3,13*,17	1,2,4,5,6,7,8,9,10,11,12,14,15,16,19,20,21,22,23
2	19,20*	1,2,4,5,6,7,8,9,10,11,13,14,15,16,21,22,23
3	23*	1,2,4,5,6,7,8,9,10,11,12,13,14,15,16,19,20,21,22
4	6*,10*	1,2,4,5,7,8,9,11,13,14,15,16,19,20,21,22,23
5	5*,11*	1,2,4,6,7,8,9,10,13,14,15,16,20,21,22,23
6	4,12*	1,2,3,7,8,9,10,11,13,14,15,16,17,19,20,21,22,23
7	18	1,2,4,6,7,8,9,10,11,12,13,14,15,16,19,20,21,22,23
8	14*	1,2,4,7,8,9,10,11,13,15,16,20,21,22,23
9	7*,8*	1,2,9,10,13,14,15,16,20,21,22,23
10	9,16	10,12,17
11	1*	13,20,21,23
12	2*,15*	1,13,14,16,20,21,22,23

\*Self-adjacent register configured as a MISR during test.

One of the barriers to implementing an economical parallel BIST architecture is self-adjacent registers. A *self-adjacent register*, marked with an asterisk in Table 2-1, is one in which at least one output of the register feeds through either a direct connection or combinational logic to at least one input of the same register (see register *R2* in Fig. 2-1a). If the self-adjacent register is configured as an LFSR in order to supply test patterns to the CLU during BIST operation, the response of the CLU cannot be observed. A self-adjacent register that is implemented with a *concurrent built-in logic block observer (CBILBO)* design as described in [Wang 86] is able to simultaneously perform both the LFSR and MISR operations because it has two sets of bistables. CBILBO register operation for a self-adjacent register is illustrated in Fig. 2-2. During normal operation, only one of the sets of CBILBO bistables is used (Fig. 2-2a). During BIST operation, the set of bistables that drives the system logic is configured into an LFSR, and the other set of

bistables is configured into a MISR. Unfortunately, the prevalence of self-adjacent registers combined with the higher hardware overhead for CBILBOs (CBILBO registers are approximately 1.75 times the size of BILBO registers) greatly increases the BIST overhead for the design in Table 2-1. When CBILBOs are not used, a self-adjacent register can be configured as a MISR during BIST operation. The MISR then provides test patterns to the CLU at the same time that it captures the response of the CLU (e.g., register  $R_2$  configured as a MISR in Fig. 2-1c). Since the state of the self-adjacent MISR depends upon its previous state and the CLU, there is no guarantee that it can generate an exhaustive set of test patterns for the CLU. Also, the CLU can adversely affect the output response capabilities of the self-adjacent MISR, as was noted by Hudson [Hudson 87] for the case when a shift operation is implemented in the CLU. We discuss the effect of the CLU on the MISR output response capabilities in detail in Sec. 4.

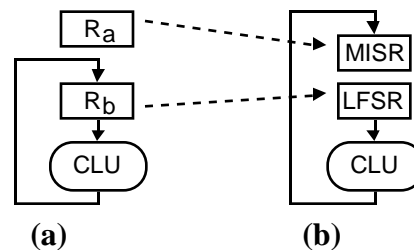


**Figure 2-2** Self-adjacent register implemented with CBILBO: (a) normal operation; (b) BIST operation.

In an effort to solve this problem, high-level synthesis techniques have been proposed that generate data path logic with a minimum number of self-adjacent registers [Avra 91], [Papachristou 91], [Mujumdar 92]. These synthesis techniques are among the first to use BIST criteria to guide the high-level synthesis of the system logic. High-level synthesis techniques that only consider area and performance during synthesis tend to generate system logic with a large number of self-adjacent registers. For example, five of the eight registers in the *Tseng* example generated by the synthesis technique described in [Tseng 86] and four of the five registers in the *DiffEq* example generated by the synthesis technique described in [Paulin 89a] are self-adjacent. The synthesis technique described in [Avra 91] generated system logic with only one self-adjacent register for both of these examples. For both examples, when CBILBO registers are used for the self-adjacent registers, the synthesis-for-BIST technique generated lower-cost parallel BIST implementations than the synthesis techniques that do not consider BIST.

Another implementation difficulty of the ideal parallel BIST architecture is determining the arrangement of system bistables into LFSRs during each test session so that each CLU tested during that test session could receive an exhaustive set of test patterns. The simplest arrangement is to configure each  $n$ -bit system register as a maximum-length LFSR, which

generates  $2^n - 1$  different test patterns (logic can easily be added to the LFSR so that it generates all  $2^n$  different patterns [McCluskey 86]). This is not an acceptable solution, however, when a single CLU is fed by multiple system registers (see *CLU2* in Fig. 2-1). In this case, the total number of different test patterns,  $P$ , that can be applied to the CLU is the least common multiple of the periods of the individual LFSRs. For  $n$  maximum-length LFSRs, where LFSR  $i$  has  $b_i$  bistables and  $b_1 \leq b_2 \leq \dots \leq b_n$ :

$$\begin{aligned} (2^{b_n} - 1) &\leq P \leq (2^{b_1} - 1)(2^{b_2} - 1)(2^{b_3} - 1) \dots (2^{b_{n-1}} - 1) \\ P &< 2^{b_1 + b_2 + b_3 + \dots + b_{n-1}} \end{aligned}$$

The maximum value for  $P$  can only be achieved when the periods of the  $n$  LFSRs are mutually prime. In data path logic, where a single CLU is often fed by  $n$   $b$ -bit system registers, we have the worst-case scenario:

$$P = 2^b - 1 \ll 2^{nb}$$

A better solution for providing a nearly exhaustive set of test patterns to each CLU is to configure the bistables on the inputs of each CLU being tested during a given test session into a single, maximum-length LFSR. Figure 2-3 illustrates this solution by showing one way to configure the registers of Fig. 2-1 into LFSRs and MISRs for each of the two required test sessions. During the first test session (Fig. 2-1b and 2-3a), registers  $R1$  and  $R2$  are configured into a single maximum-length LFSR in order to provide an exhaustive set of test patterns to *CLU4*. Registers  $R3$ ,  $R4$ , and  $R5$  are configured into a MISR to capture the output responses of *CLU3*, *CLU4*, and *CLU5*. During the second test session (Fig. 2-1c and 2-3b),  $R2$ , which is implemented with a CBILBO register, is configured with  $R3$ ,  $R4$ , and  $R5$  into a single LFSR in order to test *CLU2*. The second set of  $R2$  bistables are configured with  $R1$  into a MISR, which captures the output responses of *CLU1* and *CLU2*. The signal lines in Fig. 2-3 represent the additional interconnections required for BIST operation. Each block of feedback logic ( $f1$ ,  $f2$ , and  $f3$ ) consists of a tree of one or more exclusive-OR gates that implements the polynomial of the associated LFSR or MISR. The arrangement of the registers during BIST operation ( $R1 \rightarrow R2 \rightarrow R3 \rightarrow R4 \rightarrow R5$ ) was chosen because it minimizes the amount of BIST interconnection and feedback logic.

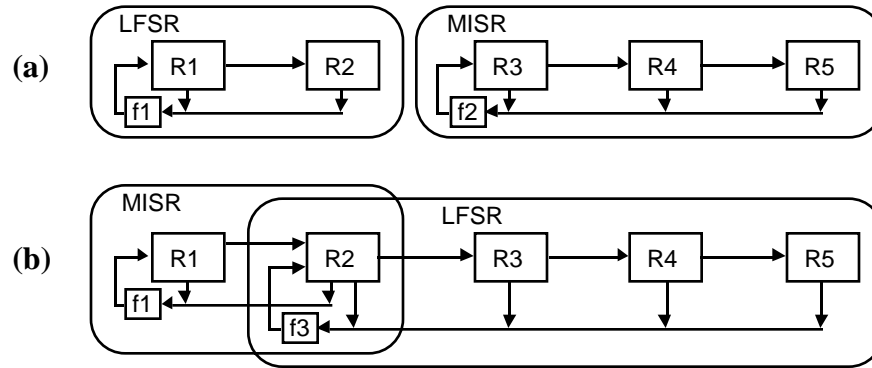


**Figure 2-3** LFSR and MISR configurations for Fig. 2-1: (a) first test session; (b) second test session.

Unfortunately, the parallel BIST architecture illustrated in Fig. 2-3 can, in practice, be extremely complicated and costly to implement. In our discussion, we have ignored how to configure LFSRs to drive the input signals (primary input signals and control signals) of the data path logic during BIST operation. Considering these signals could greatly complicate the configurations of the LFSRs during each test session, particularly if a single state machine generates all of the control signals for the data path logic. Also, Fig. 2-1 is a relatively simple data path design example. More complicated data path designs, or non-BIST scan path arrangement requirements, such as minimizing test time for deterministic stuck-at tests as described in [Gupta 91] and [Narayanan 92], could greatly increase both the hardware overhead and the total self-test time for the parallel BIST architecture. Table 2-1 provides a hint of how complicated the parallel BIST architecture could be for a real design. For example, test session seven in Table 2-1 shows that the combinational logic feeding register 18 is fed by the outputs of 19 different registers. When these 19 registers are configured into a single, maximum-length LFSR,  $2^b - 1$  different test patterns are applied to the CLU, where  $b$  is the total number of bistables in the 19 registers. Subsets of these 19 registers must be combined with other registers to create the LFSRs for the remaining eleven test sessions. As the number of test sessions increases, the BIST control logic and the LFSR interconnection logic for the design can become very complicated.

The synthesis technique described in Sec. 3 addresses one of the implementation difficulties of parallel BIST architectures by generating system logic that has a minimum number of self-adjacent registers. However, the data in Table 2-1 shows that complicated register interconnections in the system logic can greatly complicate the LFSR configurations required for a parallel BIST architecture. This issue must be addressed by synthesis techniques before extensive use of the parallel BIST architecture is practical. To that end, we have investigated more simple TPG and ORA configuration schemes, such as those found in the circular BIST

architecture. The circular BIST architecture is described in Sec. 2.2 and new synthesis techniques for this architecture are described in Secs. 4 and 5.

## **2.2 CIRCULAR BIST ARCHITECTURE**

*Circular BIST* is a low overhead, embedded BIST architecture that provides at-speed self-test operation. Circular BIST has lower area overhead than parallel BIST because it has simpler BIST control logic and interconnection logic, which also simplifies and speeds the implementation process. The circular BIST architecture was first introduced as *simultaneous self-test (SST)* by Bardell and McAnney [Bardell 82]. It was later described in slightly different forms by Stroud [Stroud 88] and Krasniewski [Krasniewski 89]. Figure 2-4 illustrates the circular BIST architecture for the data path logic in Fig. 2-1a. During BIST operation, all system bistables are configured into a single MISR as shown in Fig. 2-4b. At each clock cycle during BIST operation, the outputs of all CLUs in the design are captured in a single MISR, and the outputs of the MISR provide test patterns to the CLUs. The circular BIST architecture requires little BIST control logic since there is only one test session during which a single MISR simultaneously performs the TPG and ORA operations. The problems of register self-adjacency and LFSR configuration discussed in Sec. 2.1 for the parallel BIST architecture are not applicable to circular BIST. However, since the CLUs in the circular BIST architecture are simultaneously tested by a single, self-adjacent MISR, the pattern generation and response analysis capabilities of self-adjacent MISRs must be analyzed to ensure an effective self-test operation. These issues are discussed in Sec. 4.1 and are addressed by our synthesis for scan dependence techniques described in Secs. 4.2 and 5.

Since slightly different versions of the circular BIST architecture have been described in [Bardell 82], [Stroud 88], and [Krasniewski 89], we state here our assumptions concerning the circular BIST architecture implemented in our synthesized designs. First, we assume that all bistables in the design are included in the MISR during BIST operation. Other architectures ([Krasniewski 89], [Stroud 88]) allow some bistables to be configured in the normal mode during BIST operation in order to reduce the BIST overhead, but there is evidence that this can reduce the observability of the logic feeding those bistables [Kim 88]. Second, we assume that every system bistable is an edge-triggered flip-flop that can be configured to perform normal, shift, and MISR operations. A reset mode of operation is optional since the bistables can be controlled through the shift mode of operation. Using flip-flops simplifies the discussion of the synthesis techniques. Similar synthesis techniques can be applied if the double-latch, level-sensitive scan design method is used to implement the system bistables as described in [Bardell 82], but we do not discuss these techniques in this dissertation. Finally, we assume that the MISR feedback logic is simply a direct connection from the output of the last bistable in the MISR to the input of

the first bistable. A reconfigurable register design that supports these operations is described in Sec. 2.3.

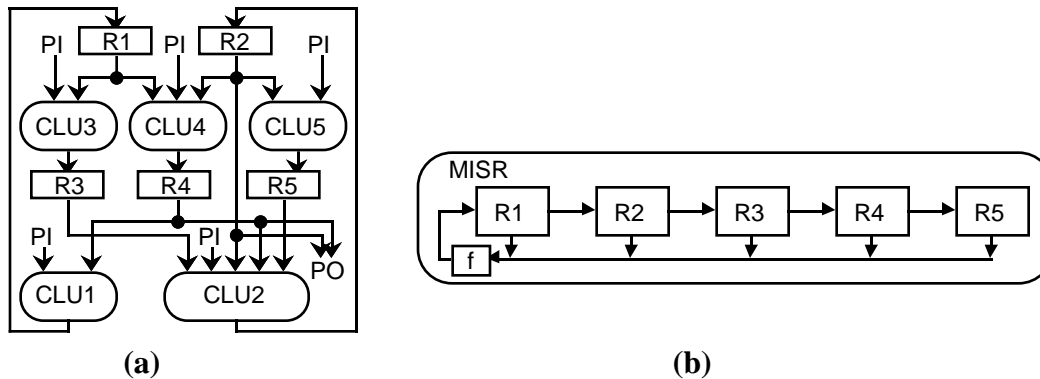


**Figure 2-4** Circular BIST architecture: (a) normal operation; (b) BIST register configuration.

### 2.3 RECONFIGURABLE REGISTER DESIGN

The distinguishing characteristic of embedded BIST architectures is that the system bistables can be configured to perform both normal operation (parallel load) as well as test operations such as serial shift, TPG, and ORA. The test operations that must be supported by each bistable depend upon the embedded BIST architecture used. The Circular Self-Test Path architecture [Krasniewski 89], for example, does not require that the system bistables perform a serial shift operation. The built-in logic block observer (BILBO) register [Konemann 79] is often used in embedded BIST architectures and implements normal, synchronous reset, serial shift, TPG, and ORA modes of operation.

Figure 2-5 illustrates a reconfigurable register design that can be used for both the parallel BIST and circular BIST architectures. The register implementation is not necessarily optimal. Its purpose is to more easily illustrate the BIST operations. In Secs. 4 and 5, we use Fig. 2-5 to illustrate scan dependence and our synthesis techniques. Figure 2-5a shows the register configuration, where each bistable in the register is implemented as shown in Fig. 2-5b. The bistable could also be implemented with a dual-port latch, such as the design specified for the SST technique [Bardell 82]. The  $Q_{i-1}$  input to the first bistable (bistable  $B_1$ ) in the register is determined by BIST mode select signal  $BIST$ , and is either the scan data input ( $SDI$ ) signal for shift operation or the output of the MISR feedback logic for MISR operation or LFSR operation. For circular BIST architectures, since a separate TPG operation is not required, signal  $BIST$  can be replaced by signal  $T_1$ , resulting in four possible modes of operation: reset, shift, normal, and MISR. Test mode select signals  $T_1$  and  $T_2$  determine the  $D$  input to each bistable in the register, as specified in Fig. 2-5c, where  $Z_i$  is the system logic input to bistable  $B_i$ .

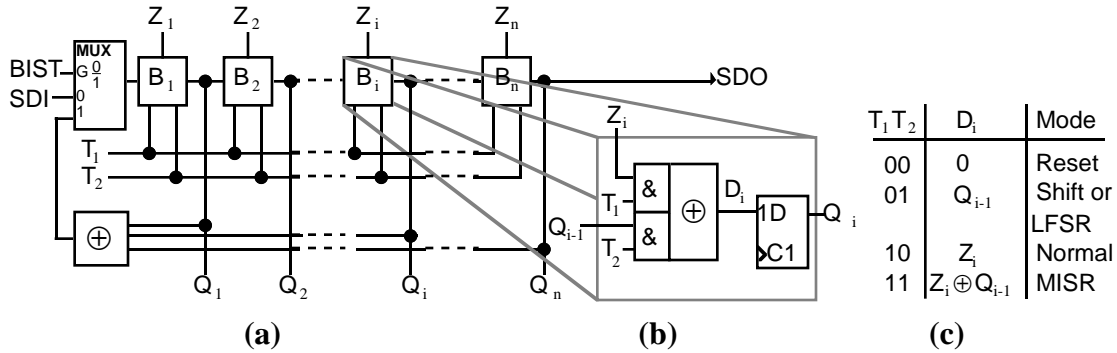


**Figure 2-5** Reconfigurable register: (a) bistable interconnections; (b) reconfigurable bistable; (c) modes of operation.

For circular BIST architectures and for parallel BIST architectures with self-adjacent registers that are not implemented with CBILBOs (i.e., for self-adjacent MISRs), the MISR operation must simultaneously provide both sufficient test patterns and accurate output response analysis. It has been proven that, when the  $Z$  inputs are independent of the state of an  $n$ -bit MISR, the MISR generates test patterns that are similar in behavior to random patterns [Krasniewski 89], [Kim 88]. Specifically, as  $P$  goes to infinity, where  $P$  is the number of test patterns applied during BIST operation, the probability of the MISR being in any one of the  $2^n$  possible states is  $2^{-n}$ . The  $Z$  inputs to a self-adjacent MISR, however, are a function of the state of the MISR. Simulation results presented in [Kim 88] and [Stroud 88] indicate that the MISR test pattern characteristics are not significantly different from random patterns when the  $Z$  inputs depend upon the state of the MISR. It is not clear whether a MISR implemented with a primitive polynomial [Kim 88] produces any better patterns than a MISR implemented with a single  $Q_n$  feedback connection [Krasniewski 89].

Figure 2-6a shows a portion of the reconfigurable register during MISR operation to illustrate its error capture capabilities. During MISR operation, the input to each bistable,  $D_i$ , is the exclusive-OR of the output of the previous bistable in the MISR,  $Q_{i-1}$ , and the system logic input to the bistable,  $Z_i$ . At each clock cycle, an error in either  $Z_i$  or  $Q_{i-1}$  is observable at  $D_i$  (i.e., captured in bistable  $B_i$ ) regardless of the state of the error-free signal. Figure 2-6b is a truth table for signals  $D_i$  ( $D_i = Q_{i-1} \oplus Z_i$ ) and  $DE_i$  ( $DE_i = QE_{i-1} \oplus Z_i$ ), where  $QE_{i-1}$  is the faulty version of signal  $Q_{i-1}$ . Figure 2-6b shows that, regardless of the state of signal  $Z_i$ ,  $D_i$  differs from  $DE_i$ , so when  $Z_i$  is fault-free, an error in  $Q_{i-1}$  is always captured in bistable  $B_i$ . Because the exclusive-OR operation is symmetric, the same is true when  $Q_{i-1}$  is fault-free and  $Z_i$  is faulty. However, errors in both signals  $Z_i$  and  $Q_{i-1}$  in a single clock cycle are not observable at  $D_i$ . Thus, once captured in a bistable of the MISR, an error is transferred from one bistable ( $Q_{i-1}$ ) to the next ( $Q_i$ ) at each clock cycle as long as it is not masked by a simultaneous error in the corresponding system logic

input signal  $Z_i$ . In addition, the error may be transferred to other bistables in the MISR through the MISR feedback logic or, if the MISR is self-adjacent, through the system logic.

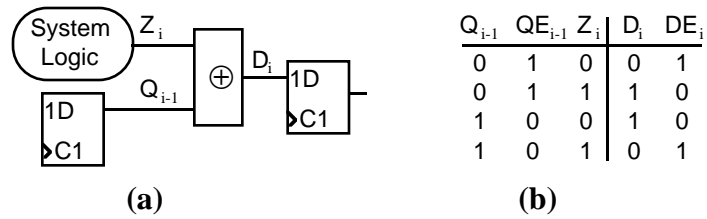


**Figure 2-6** MISR error capture capabilities: (a) MISR configuration; (b) error response.

### 3 ALLOCATION AND BINDING FOR PARALLEL BIST

The interconnection of system logic registers can greatly affect the area overhead of parallel BIST architectures and the effectiveness of the TPGs and ORAs as was shown in Sec. 2.1. System register interconnect is an issue that must be addressed during high-level synthesis, when variables in the behavioral description are mapped to specific registers in the structural description. Little work has been done in the area of high-level synthesis-for-testability. Recently, high-level synthesis algorithms for non-scan and partial-scan architectures have been given [Lee 93]. These algorithms are not well-suited for parallel BIST architectures, however, because they favor the generation of self-adjacent registers since self-adjacent bistables, which can occur in self-adjacent registers, are considered easier to test by sequential automatic test pattern generation tools [Cheng 89]. High-level synthesis procedures that discourage the generation of self-adjacent registers are described in [Avra 91], [Papachristou 91], and [Mujumdar 92]. The technique described in [Papachristou 91] generates data path logic with no self-adjacent registers, but may increase the latency of the functional operation in order to do this. The module and register binding algorithm given in [Mujumdar 92] discourages, but does not prevent, the generation of self-adjacent registers.

This section provides an overview of our high-level synthesis-for-BIST technique, first described in [Avra 90], that takes as input a scheduled data flow description of the system logic and, without increasing the latency of the description, generates a parallel BIST data path structure with a minimum number of self-adjacent registers. A more detailed description of the technique is given in [Avra 91]. The synthesis procedure consists of first mapping the input data flow description to a register conflict graph. The nodes of the graph are then colored using a node coloring algorithm that is guided by design implementation costs such as interconnection area and multiplexer size. Finally, the colored graph is mapped to hardware. A simple constraint imposed on the register conflict graph prevents the register binding algorithm from creating self-adjacent registers in the generated data path logic, thereby reducing the area overhead of the parallel BIST architecture when self-adjacent registers are implemented with CBILBO registers. We also incorporate a novel register allocation technique that allows the register binding algorithm increased flexibility in synthesizing an efficient hardware implementation.

Section 3.1 is background material and provides an overview of the operations performed during high-level synthesis. In Sec. 3.2, we describe the register conflict graph, focusing on the features that make our high-level synthesis procedure unique. Section 3.3 describes the register binding algorithm that is implemented in our synthesis tool and compares designs generated by our tool with designs generated by other synthesis techniques. Section 3.4 summarizes our contributions in high-level synthesis for parallel BIST.

### 3.1 HIGH-LEVEL SYNTHESIS TASKS

Register binding is one of several tasks performed during high-level synthesis. We use Fig. 3-1 to illustrate the high-level synthesis operations of scheduling, allocation, and binding. More detailed information on these and additional high-level synthesis operations can be found in [De Micheli 94]. High-level synthesis operations are typically applied to a data flow graph (Fig. 3-1b) that represents a behavioral description of the system operation (Fig. 3-1a). Nodes and edges in the data flow graph correspond to operations and variables, respectively, in the behavioral description. *Scheduling* consists of assigning the operations in the data flow description to execute in certain clock cycles. For example, Fig. 3-1b shows that two addition operations are performed in the first clock cycle, while one addition and one multiplication are performed in the second clock cycle. Clock cycle boundaries in Fig. 3-1b are delimited by dotted lines. The scheduling algorithm may generate a schedule that, given a hardware constraint, executes in a minimum number of clock cycles or that, given a timing constraint, requires a minimum number of function blocks to perform the operations in the behavioral description. *Allocation* consists of determining the number of hardware resources necessary to implement the data flow description. Two addition function blocks (for  $+_1$  and  $+_2$ ), one multiplication function block, and five registers (represented by squares on the edges of the graph) have been allocated for the data flow graph in Fig. 3-1b. During *binding*, operations in the data flow graph are mapped to specific instances of hardware function blocks (*ADD1*, *ADD2*, and *MULT* in Fig. 3-1c), variables that exist at clock cycle boundaries are mapped to registers (rectangles in Fig. 3-1c), and multiplexers and buses are generated to accommodate the required flow of data. Our register allocation and binding techniques differ from existing techniques in two ways: 1) we incorporate a simple constraint in the binding of variables to registers such that the number of self-adjacent registers is minimized, and 2) to compensate for this constraint, we incorporate a register allocation technique that increases the flexibility of the register binding procedure.

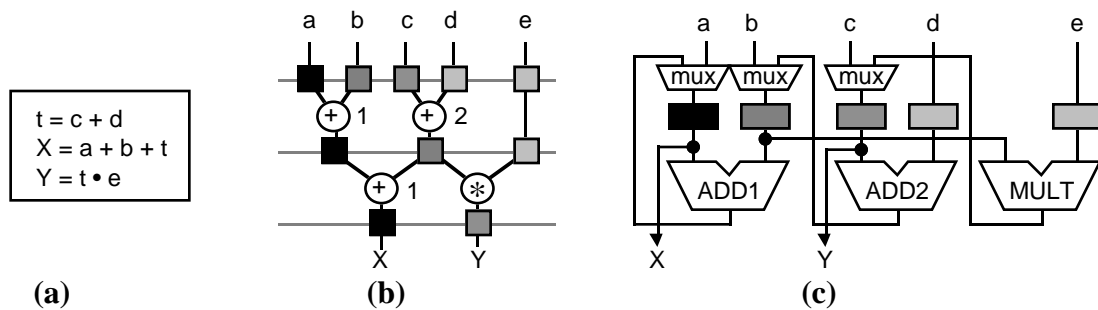


**Figure 3-1** High-level synthesis example: (a) data flow description; (b) scheduled, bound data flow graph; (c) data path logic.

### 3.2 REGISTER CONFLICT GRAPH

Our register allocation and binding operations are applied to a register conflict graph data structure. Each node in the register conflict graph represents an edge from the data flow graph that crosses a clock cycle boundary. An edge between two nodes in the register conflict graph indicates that the two variables associated with those nodes cannot be stored in the same register. *Register binding* consists of assigning a color to each of the nodes in the register conflict graph such that adjacent nodes have different colors. All nodes with the same color can be mapped to the same register in the final implementation. This is analogous to the techniques described in [Tseng 86] and [Paulin 89b], where a *register compatibility graph* is created, clique partitioning is performed, and all nodes in the same clique are assigned to the same register. Figure 3-2b illustrates the typical conflict graph-based register allocation and binding procedures for the data flow graph of Fig 3-1b. Figure 3-2a is the same data flow graph as Fig. 3-1b except that the register binding information (colored squares on clock cycle boundaries) has been removed. Nine nodes, corresponding to data flow graph variables  $a, b, c, d, e, s, t, X,$  and  $Y$ , are created in the register conflict graph. Edges are added between nodes whose variables cannot be assigned to the same register. For example, variables  $a, b, c, d,$  and  $e$  all exist at the first clock cycle in the data flow graph and must therefore all be assigned to different registers, so their nodes form a clique in the register conflict graph. One possible coloring of the register conflict graph is shown in Fig. 3-2b, where the different colors correspond to different registers in the structural implementation.

We define *register allocation* as the method used to determine how many nodes to create in the register conflict graph. Our register allocation procedure is illustrated in Fig. 3-2c and is unique in that it creates multiple nodes in the register conflict graph for a single variable in the data flow graph under three conditions: delayed values, multiple targets, and multiple sources. We do this in order to increase the flexibility of the register binding algorithm in mapping variables to non-self-adjacent registers. For the *delayed values* situation, a node is added to the register conflict graph for each clock cycle in a variable's lifetime. This means that the variable could be transferred from one register to another rather than held in a single register for its entire lifetime as most register allocation techniques require. The delayed values allocation scheme is illustrated by nodes  $e$  and  $De$  in Fig. 3-2c, which both represent variable  $e$  from the data flow description. Note that there is no edge between nodes  $e$  and  $s$  since they exist at different clock cycles, but there is an edge between nodes  $De$  and  $s$ . The delayed values consideration is an extension of the technique first introduced in [Paulin 89b], where it was shown that when a register is allocated for the first clock cycle of a variable's lifetime, and another register is allocated for the remaining clock cycles of its lifetime, interconnect cost can sometimes be reduced. *Multiple targets* means that a node is added to the register conflict graph for each

output of an operation that crosses a clock cycle boundary. For example, nodes  $t1$  and  $t2$  in Fig. 3-2c both represent the variable  $t$  in Fig. 3-2a. Node  $t1$  represents the input to the addition operation, and node  $t2$  represents the input to the multiplication operation. No edge is added between nodes  $t1$  and  $t2$  because they could be assigned to the same register since they represent the same variable. *Multiple sources*, which is not shown in Fig. 3-2c, is similar to multiple targets except that a node is added to the conflict graph for each operation input that represents a single variable. This situation occurs when the input to an operation is assigned a value in multiple, mutually-exclusive branches of a conditional statement. The multiple sources situation is described in detail in [Avra 91].

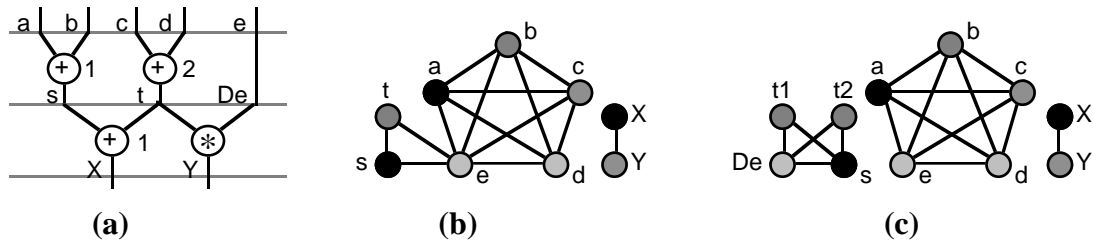


**Figure 3-2** Register conflict graph example: (a) data flow graph from Fig. 3-1b; (b) typical register conflict graph; (c) our register conflict graph.

*Conflict edges* are edges in the register conflict graph that specify that the variables associated with the adjacent nodes cannot be assigned to the same register. We call the edges shown in the register conflict graphs in Fig. 3-2 *schedule conflict edges* because the conflict that exists between the adjacent nodes is due to the schedule specified for the data flow graph. Schedule conflict edges therefore maintain the functionality of the system logic. Our register binding algorithm is unique in that we include an additional type of conflict edge in the register conflict graph that maintains the testability of the generated system logic. *Testability conflict edges* are added between two nodes when one node represents a variable that is an input to a function block and the other node represents a variable that is an output of the same function block. For example, Fig. 3-3b is the register conflict graph for Fig. 3-3a, showing just the testability conflict edges for the three function blocks,  $+_1$ ,  $+_2$ , and  $*$ . Note that an edge is added between nodes  $a$  and  $s$  and between nodes  $a$  and  $X$  because both  $s$  and  $X$  are outputs of the same function block. Node  $e$  has no adjacent testability conflict edges because it is not an input or an output of any function block. Testability conflict edges require that the inputs and the outputs of a function block be assigned to different registers, and this guarantees that no self-adjacent registers will be synthesized. One situation requires the use of a self-adjacent register: when two operations in consecutive clock cycles in the data flow graph are assigned to a single function block and the output of one operation is the input to the other (see variable  $s$  in Fig. 3-3a). In this case, the node that is associated with both the input and the output of the function block is

identified by a self-edge in the register conflict graph and must be assigned to a CBILBO register.

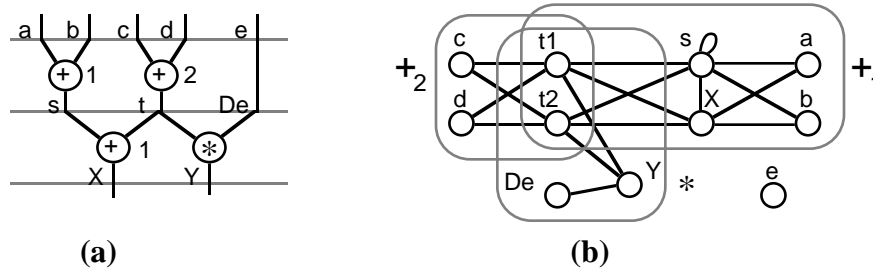


**Figure 3-3** Testability conflict edges: (a) data flow graph; (b) register conflict graph with testability conflict edges.

*Cost edges* are weighted edges that are added between certain compatible nodes (nodes that do not already have a conflict edge between them) in the register conflict graph, and are used to guide the graph coloring algorithm toward the lowest-cost design. A positive weight is assigned to the cost edge if it is not advantageous to assign the same color to the adjacent nodes, and a negative weight is assigned if it is advantageous. For example, negative-weight cost edges are added between nodes  $a$  and  $t1$ , and between  $b$  and  $t1$  in Fig. 3-3b because they represent variables that are inputs to a single function block ( $+_1$ ) in two different clock cycles. Interconnection and multiplexer cost will be lower if these two variables are assigned to the same register.

### 3.3 IMPLEMENTATION AND RESULTS

We have implemented our register allocation and binding algorithm for parallel BIST designs in the synthesis tool described in Sec. 6. Given a behavioral VHDL [IEEE 88] description of the design, the tool first creates a data flow graph, then performs scheduling and operation allocation and binding as described in Sec. 6.4, and then creates the register conflict graph as described in Sec. 3.2. We have implemented a modified version of the Brelaz node coloring algorithm [Turner 88] to perform the register binding operation. The pseudo-code for our register binding algorithm is given in Table 3-1. The algorithm attempts to color the nodes in the register conflict graph with the minimum number of colors in order to minimize the number of registers in the generated design. Since solving the general node coloring problem is NP-complete, we use heuristics to sort the uncolored nodes, then color the node with the highest priority. The node to be colored is assigned the same color as a node that is adjacent via the lowest, negative-weight cost edge. If the node to be colored has no adjacent negative-weight cost edges, the algorithm tries to assign it the same color as a non-adjacent node. After a node is colored, the characteristics of the adjacent, uncolored nodes are updated, and all of the uncolored nodes are sorted to find the next node to color.

**Table 3-1** Register binding algorithm for parallel BIST register conflict graph.

---

```

Color_Nodes (Register Conflict Graph)
While (Some Nodes Uncolored) do
  Sort Uncolored Nodes According to:
    1. Has Self-Adjacent Constraint Edge
    2. Has Least Number Available Colors
    3. Has Most Constraint Edges
    4. Has Least Sum Of Cost Edges
  Select Highest-Priority Node
  Color With Lowest-Cost Adjacent Color
  Update Uncolored, Adjacent Nodes
end While

```

---

The data path logic in Fig. 3-1c was generated by applying the register binding algorithm in Table 3-1 to the data flow graph in Fig. 3-1b. As shown by the self-edge in Fig. 3-3b, node  $s$  must be assigned to a self-adjacent register, so the register binding algorithm selected node  $s$  to color first. The register associated with node  $s$  (and nodes  $a$  and  $X$  since they were assigned the same color) is implemented as a CBILBO register and is the only self-adjacent register in the generated design.

Table 3-2 compares the results of our register allocation and binding technique, called *RALLOC*, with the results published in [Tseng 86], [Pangrle 88], [Paulin 89a], and [Papachristou 91] for two design examples, *Tseng* [Tseng 86] and *DiffEq* [Paulin 89a]. The design cost estimates of the synthesized hardware are based on the number of self-adjacent (*SA*) registers, non-self-adjacent (*NSA*) registers, multiplexer inputs (*mux*), interconnections (*int*), and control signals (*ctl*), and are computed as follows:

$$\begin{aligned} \text{cost}_1 &= 14 \cdot (\text{NSA reg}) + 14 \cdot (\text{SA reg}) + \text{mux} + \text{int} + \text{ctl} \\ \text{cost}_2 &= 20 \cdot (\text{NSA reg}) + 35 \cdot (\text{SA reg}) + \text{mux} + \text{int} + \text{ctl} \end{aligned}$$

For the first design cost estimate,  $\text{cost}_1$ , all registers have the same cost. This represents the cost of data path logic with no BIST or scan circuitry. The second design cost estimate,  $\text{cost}_2$ , represents the cost of a parallel BIST implementation of the data path logic. In this case, non-self-adjacent registers are implemented with the register design shown in Fig. 2-5a, which is estimated to be approximately 20 times the cost of a multiplexer input, and self-adjacent registers are implemented with the higher-cost CBILBO register.

The goal of the synthesis techniques presented in [Tseng 86], [Pangrle 88], and [Paulin 89a] is to minimize the area of the generated data path logic. Since they do not consider testability during the synthesis process, their implementations, understandably, have a higher number of self-adjacent registers, which partially accounts for the higher values for  $\text{cost}_2$  in Table 3-2. Both our synthesis technique and the technique described in [Papachristou 91] attempt to minimize the cost of the design while preventing the generation of self-adjacent registers. By comparing our

technique with techniques that do not consider testability, we show the difference between *synthesis-for-BIST*, where the design is optimized for a particular BIST architecture, and *BIST synthesis*, where BIST circuitry is added to a design that has been synthesized for area and performance.

For both examples in Table 3-2, our technique generated the lowest-cost parallel BIST implementation ( $cost_2$ ). Our technique also generated designs with the minimum number of registers, showing that the additional testability constraint edge in the register conflict graph did not require an increase in the number of registers for these examples. The  $cost_1$  column in Table 3-2 shows that, if parallel BIST is not implemented, the costs of the data path designs generated by our technique are comparable to the costs of the other designs.

**Table 3-2** Comparison of synthesis procedures on *Tseng* [Tseng 86] and *DiffEq* [Paulin 89a] data flow descriptions.

Name	NSA reg	SA reg	mux	int	ctl	$cost_1$	$cost_2$
<i>Tseng</i>							
[Tseng 86]	3	5	15	31	23	181	304
[Pangrle 88]	4	3	11	26	18	153	240
[Papachristou 91]	8	0	12	28	20	172	220
RALLOC	4	1	16	29	21	136	181
<i>DiffEq</i>							
[Pangrle 88]	1	5	17	34	23	158	269
[Paulin 89a]	1	4	19	35	24	148	238
RALLOC	4	1	22	38	27	157	202

### 3.4 CONTRIBUTIONS

We have developed and implemented a new register allocation and binding technique that generates data path logic optimized for the parallel BIST architecture given a scheduled, operation-bound data flow description of the design. A simple testability constraint edge added to the register conflict graph is used to guarantee that the generated data path logic has a minimum number of self-adjacent registers. This testability requirement can be easily adapted to existing register allocation and binding procedures. We have also developed and implemented new techniques for register allocation (delayed values, multiple targets, and multiple sources) that provide the register binding procedure increased flexibility in synthesizing an efficient hardware implementation while minimizing the number of self-adjacent registers.

Results show that, when the parallel BIST architecture is used, addressing register self-adjacency during high-level synthesis results in a lower-cost design. For both examples evaluated, our technique synthesized the lowest-cost, parallel BIST design. In addition, for both

examples, if parallel BIST is not implemented, the costs of the data path designs generated by our technique are comparable to the costs of the other designs. This shows that, even if BIST and scan circuitry is not included in the design, minimizing the number of self-adjacent registers during synthesis does not necessarily increase, and may even reduce, the cost of the generated data path logic.

## 4 SYNTHESIS FOR SCAN DEPENDENCE

Performance degradation, area overhead, and *test transparency* (the fraction of defects not detected by the test) are three issues that must be addressed when synthesizing a built-in self-testable design. The register allocation and binding technique described in Sec. 3 reduces the area overhead of a parallel BIST design without increasing test transparency or the number of clock cycles required to execute the data path function. However, since there is additional BIST logic associated with each system register in the data path, the clock period may have to be increased, resulting in slower performance. In this section, we describe a new synthesis technique, applied to the bistables in the design, that relies on the sharing of system logic and test logic to reduce the area and improve the performance without increasing the test transparency of BIST architectures, such as circular BIST and parallel BIST, that make use of embedded MISRs. This technique was first described in [Avra 93]. A more detailed description of the technique is given in [Avra 94a].

The goal of our synthesis technique is to arrange the system bistables into scan paths so that some of the BIST and scan logic is shared with the system logic. Logic sharing is possible when *scan dependence* is introduced in the design. Other BIST design techniques attempt to avoid all types of scan dependence because it can increase the test transparency of embedded MISRs. We show that introducing certain types of scan dependence in embedded MISRs can reduce the overhead and the test transparency, and we describe a synthesis technique that maximizes the amount of this *beneficial* scan dependence. The synthesis technique first analyzes the CUT feeding the MISR, then based on the CUT function, it modifies the MISR function in order to reduce the amount of aliasing during BIST operation. We have implemented this synthesis technique in our synthesis-for-test design tool (described in Sec. 6) and we present fault simulation, layout area, and delay results for circular BIST versions of benchmark circuits that have been synthesized with our technique.

Section 4.1 provides a formal definition of scan dependence and includes design examples that illustrate its advantages and disadvantages. In Sec. 4.2, we describe design techniques for beneficial scan dependence and show how to introduce it in the design by arranging the system bistables into MISRs. Section 4.3 contains fault simulation and overhead results of several benchmark circuits generated with our synthesis technique and optimized for the circular BIST architecture described in Sec. 2.2. Section 4.4 summarizes our contributions in the area of scan dependence.

#### 4.1 SCAN DEPENDENCE

A system bistable  $B_i$  that can be reconfigured to perform scan operation is *scan dependent* if and only if its system logic input signal,  $Z_i$ , is functionally dependent on the bistable that immediately precedes it in the scan path. For example, assume that the system logic input to bistable  $B_5$  is the function  $Z_5 = Q_1 Q_3 + Q_2 Q_4$ . If any of the bistables  $B_1 - B_4$  immediately precede  $B_5$  in the scan path, bistable  $B_5$  is scan dependent on that preceding bistable. If, however, bistable  $B_6$  immediately precedes  $B_5$  in the scan path,  $B_5$  is not scan dependent since  $Z_5$  is not a function of  $Q_6$ . Bhatia [Bhatia 93] showed that scan dependence can be used to reduce the area overhead of certain types of scan architectures. We showed in [Avra 93] that some types of scan dependence can be used to reduce the overhead and improve the effectiveness of embedded BIST architectures.

Figure 4-1 illustrates a problem that can occur in embedded MISRs if the type of scan dependence is not identified when arranging bistables in the scan path. In this example, the system logic input to bistable  $B_2$  is the function  $Z_2 = Q_1 + f$ , where  $f$  is an output of combinational logic (CLU), the inputs to which are primary inputs (PIs) and bistable outputs excluding the output of bistable  $B_1$  (DFFs). When bistable  $B_2$  is implemented as shown in Fig. 2-5b, the function of its  $D$  input during MISR mode ( $T_1 = 1, T_2 = 1$ ) is  $D_2 = Q_1 \oplus (Q_1 + f) = Q_1 f$ , as shown in Fig. 4-1b. The problem with this function is that it greatly reduces the number of errors that the MISR can capture during MISR operation. An error previously captured by the MISR and located at bistable  $B_1$  will only remain in the MISR (via transfer to bistable  $B_2$ ) when  $f = 1$ . Similarly, an error in  $f$  is only captured in the MISR when  $Q_1 = 0$ .

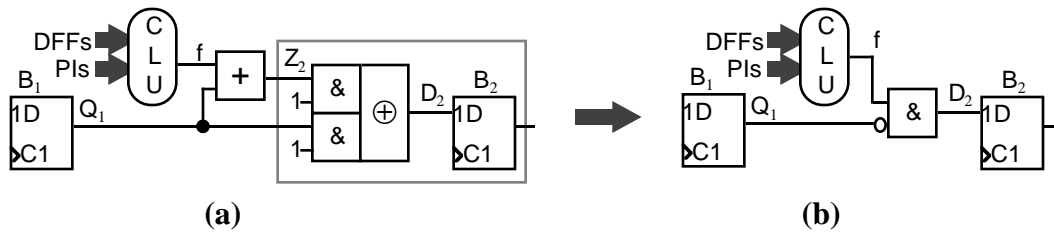


**Figure 4-1** Embedded MISR with scan dependence: (a) implementation; (b) MISR operation.

In order to determine whether or not scan dependence could be a significant problem in embedded BIST architectures, we implemented the circular BIST architecture, as described in Sec. 2.2, on three of the ACM/SIGDA LGSynth91 benchmark circuits [ACM/SIGDA 91]. For each circuit, the order of the bistables in the MISR was selected to maximize the number of scan dependent bistables in order to represent a worst-case scenario. We then fault-simulated BIST operation, using the bistable outputs as observation points. For each circuit, BIST operation was first executed until all of the single stuck-at faults in the circuit had been captured at least once in

the MISR (i.e., *detected* by the BIST operation). The number of BIST operation clock cycles,  $P$ , required to detect 100% of the single stuck-at faults varies from circuit to circuit, depending upon the testability of the combinational logic, and from simulation to simulation, depending upon the initial state of the bistables. To determine a value for  $P$ , we ran five fault simulations on the combinational logic portion of each circuit, applying test patterns randomly-generated by the fault simulator to the inputs of the circuit. We chose  $P$  to be equal to the average number, over the five simulations, of randomly-generated test patterns required to detect all single stuck-at faults in the combinational logic. We then fault-simulated the BIST operation of the entire circuit (combinational logic plus bistables) for  $P+90$  clock cycles, observing the states of all of the bistables during the last 90 clock cycles. The fault simulation results of these 90 clock cycles are shown in Fig. 4-2. At each clock cycle, the percentage of faults that alias is the percentage of faults for which the states of the bistables in the faulty and fault-free circuits are identical. Our motivation for performing the experiment in this manner is that, in practice, BIST operation would probably be terminated, and the test response shifted out, at some point during that window of 90 clock cycles. Figure 4-2 shows that, even though the TPG function of the BIST architecture is sufficient to detect all single stuck-at faults, there is a significant chance that a faulty circuit will not be identified due to aliasing in the ORA function. For example, if BIST operation is halted and the state of the circuit is observed at clock cycle  $P+40$ , there is a probability of approximately 40% for *mult32b*, 25% for *mult16b*, and 10% for *s641* that the faulty circuit will be indistinguishable from the fault-free circuit. We show in Sec. 4.3.2 that these probabilities are approximately zero for the same circuits if there is no scan dependence in the design.

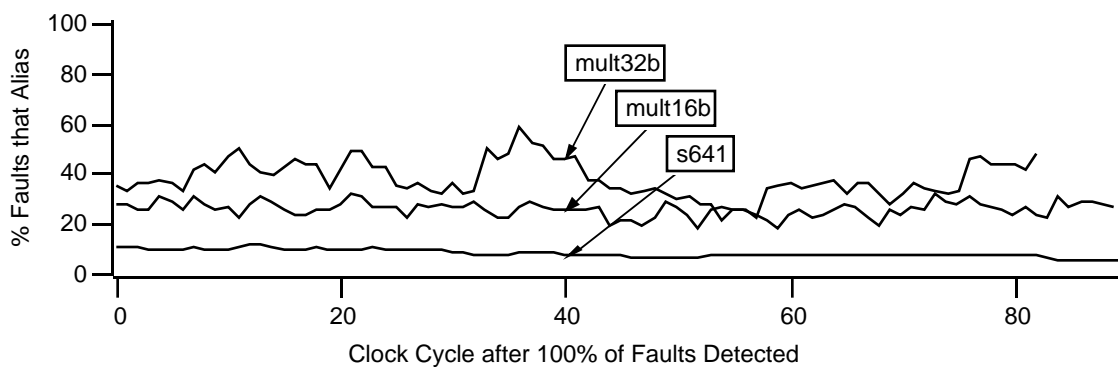


**Figure 4-2** Fault simulation results of BIST operation of circular BIST circuits with maximum scan dependence.

One way to address the scan dependence problem is to arrange the bistables in the MISR such that a minimum number of bistables are scan dependent [Stroud 88], [Pilarski 92]. For example, in order to eliminate scan dependence for bistable  $B_2$  ( $Z_2 = Q_1 + f$ ) in Fig. 4-1, neither  $B_1$  nor any of the bistables whose outputs are inputs to function  $f$  can immediately precede  $B_2$  in

the MISR. Unfortunately, it may not always be possible to create an embedded MISR that has no scan dependent bistables, particularly in “control-dominated” designs where bistable inputs are often a function of a significant number of the bistable outputs in the design. Also, eliminating all scan dependence eliminates opportunities to share system and test logic.

We propose to solve the problem of MISR aliasing due to scan dependence by using a different MISR mode function for the scan dependent bistables. The MISR function used depends upon the type of scan dependence. For example, when the system logic for bistable  $B_2$  has the general form  $Z_2 = Q_1 + f$ , where  $B_1$  immediately precedes  $B_2$  in the MISR, we use  $Q_1 \oplus f$  as the MISR function. The Boolean function for the input to  $B_2$  is then:

$$\begin{aligned} D_2 &= T_1' T_2' Q_1 + T_1' T_2 Q_1 + T_1 T_2' (Q_1 + f) + T_1 T_2 (Q_1 \oplus f) \\ &= T_1' Q_1 + T_1 T_2' (Q_1 + Q_1 f) + T_1 T_2 (Q_1 \oplus f) \\ &= Q_1 (T_1' + T_2' + f) + Q_1 (T_1 f) \end{aligned}$$

One possible logic implementation for this function is compared with a scan dependence avoidance implementation in Fig. 4-3. Figure 4-3a shows our implementation, where the MISR function is  $D_2 = Q_1 \oplus f$ . The scan dependence avoidance implementation is shown in Fig. 4-3b, where the MISR function is  $D_2 = Q_x \oplus Z_2 = Q_x \oplus (Q_1 \oplus f)$ ,  $Q_x$  is the output of another bistable in the scan path, and  $f$  is not a function of  $Q_x$ . Both implementations were mapped to LSI Logic 1.0 micron standard cell gates [LSI 91]. Area (in LSI Logic cell units) and delay ( $f$  to  $D_2$  in nanoseconds) for the shaded areas of Fig. 4-3 are provided in Table 4-1. Note that the circuit in Fig. 4-3a performs the shift operation ( $D_2 = Q_1$ ) when  $T_1 = T_2 = 0$ , whereas the circuit in Fig. 4-3b performs a synchronous reset operation ( $D_2 = 0$ ). Note also that bistable  $B_2$  in Fig. 4-3a has greater observability of system logic errors during MISR mode than bistable  $B_2$  in Fig. 4-3b. If bistable  $B_2$  is not scan dependent, an error observable at  $f$  is only captured in the MISR when  $Q_1$  is 0 (i.e., when the error is observable at  $Z_2$ ), whereas if scan dependence is implemented as shown in Fig. 4-3a, all errors observable at  $f$  are captured in the MISR. Greater observability of system logic errors can reduce the test transparency of the BIST operation.

The disadvantage of scan dependence, as shown in Fig. 4-2, is that it can result in significant error loss in embedded MISRs if the function for MISR mode is not specifically selected for the type of scan dependence. The advantage of scan dependence, as shown in Fig. 4-3, is that, when the MISR function is carefully selected, the delay and area of the test logic for the scan dependent bistable can sometimes be reduced. Section 4.2 summarizes our synthesis technique, which first analyzes the combinational logic feeding each system bistable, then based on this analysis, determines the best arrangement of bistables into MISRs and modifies the MISR function in order to reduce the amount of aliasing during BIST operation.

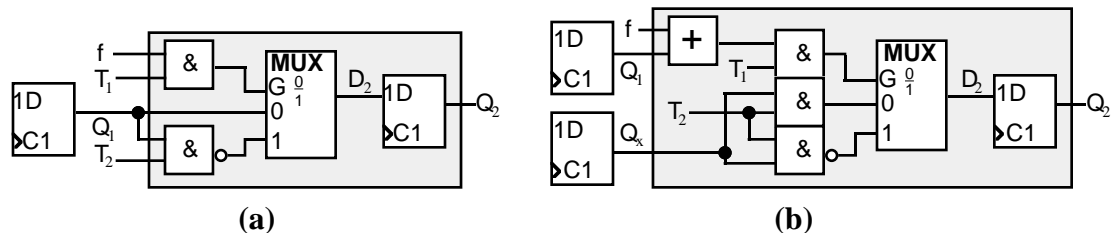


**Figure 4-3** Scan dependence solutions for  $Z_2 = Q_1 + f$ : (a) our technique:  $D_2 = Q_1 \oplus f$  during MISR operation; (b) avoiding scan dependence:  $D_2 = Q_x \oplus (Q_1 \oplus f)$  during MISR operation.

**Table 4-1** Area and delay for shaded logic in Fig. 4-3 based on data in [LSI 91].

Circuit	Area (CUs)	$f \rightarrow D_2$ Delay (ns)
Fig. 4-3a	33	1.88
Fig. 4-3b	41	2.21

#### 4.2 SYNTHESIS FOR SCAN DEPENDENCE

Scan dependence that may be beneficial for embedded MISRs must be identified early in the design cycle since it can affect how the system logic is implemented, as was illustrated in Fig. 4-3. Rather than analyzing a structural description of the system logic, the synthesis technique must analyze the system logic Boolean equation for each system bistable to determine whether or not scan dependence is beneficial, and if so, to select the appropriate test mode functions. We use Shannon decomposition to transform each system logic equation,  $Z_j$ , into a form that can be easily analyzed for scan dependence, and if beneficial for embedded BIST, synthesized into an efficient structural implementation. *Shannon decomposition* of a Boolean equation  $Z_j(Q_1, Q_2, \dots)$  with respect to variable  $Q_1$  results in:

$$Z_j(Q_1, Q_2, \dots) = Q_1 Z_j(1, Q_2, \dots) + \bar{Q}_1 Z_j(0, Q_2, \dots)$$

where  $Z_j(1, Q_2, \dots)$  is the  $Q_1$ -residue and  $Z_j(0, Q_2, \dots)$  is the  $\bar{Q}_1$ -residue of  $Z_j$ . For each  $Q_i$  that is essential for system logic equation  $Z_j$ ,  $i \neq j$ , we perform Shannon decomposition on  $Z_j$  with respect to  $Q_i$ . Then, based on the values of the residues, we classify  $Q_i$  as one of four cases according to Table 4-2, where “constant” is either logic 0 or logic 1, and  $Q_i^*$  is either  $Q_i$  or  $Q_i'$ .  $Q_i$  is *essential* for  $Z_j$  if and only if all sum-of-products expressions for  $Z_j$  include either  $Q_i$  or  $Q_i'$  or both. If  $Q_i$  cannot be classified as case 1, case 2, or case 3, it is classified as case 4. Cases 1, 2, and 3 are considered beneficial scan dependence because, when using the MISR function given in Table 4-2, they can be implemented with less logic than if scan dependence is avoided and the MISR function  $Q_k \oplus Z_j$  is used. Figure 4-4 shows possible logic implementations for representative functions of cases 1, 2, and 3.

**Table 4-2** Scan dependence classification of decomposed Boolean equations.

Class	$Q_i$ -residue	$Q_i'$ -residue	Equation Form	MISR Function
Case 1	constant	constant	$Z_j = Q_i^*$	$D_j = Q_i^*$
Case 2	constant not constant	not constant constant	$Z_j = (Q_i^* + f)^*$	$D_j = Q_i^* \oplus f$
Case 3	$(Q_i' \text{-residue})'$	$(Q_i \text{-residue})'$	$Z_j = Q_i^* \oplus f$	$D_j = Q_i^* \oplus f$
Case 4	not constant	not constant	$Z_j = Q_i f + Q_i' g$	AVOID

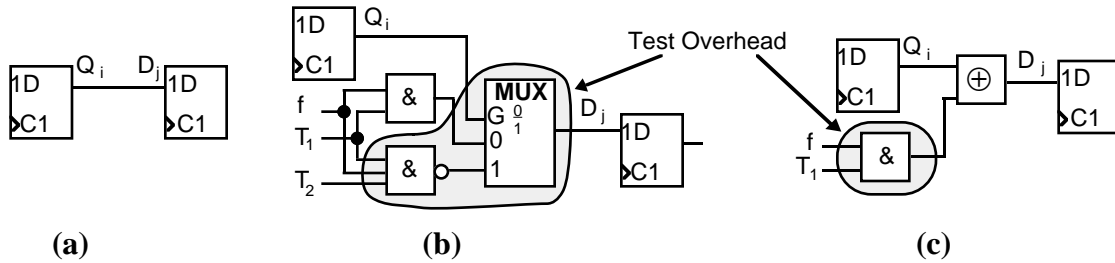


**Figure 4-4** Beneficial scan dependence implementations: (a) case 1:  $Z_j = Q_i$ ; (b) case 2:  $Z_j = Q_i + f$ ; (c) case 3:  $Z_j = Q_i \oplus f$ .

To date, we have not determined a way for system logic equations classified as case-4 equations to benefit, in terms of reduced area and performance overhead, from scan dependence. Therefore, if the Shannon decomposition of  $Z_j$  with respect to  $Q_i$  is a case-4 equation, bistable  $B_i$  should not immediately precede bistable  $B_j$  in the scan path, otherwise the effectiveness of the MISR will be compromised. To show that this is true, let  $p$  and  $q$  be the  $Q_i$ - and  $Q_i'$ -residues, respectively, of  $Z_j$  ( $Z_j = Q_i p + Q_i' q$ ), and let  $B_i$  immediately precede  $B_j$  in the scan path. If  $B_j$  is implemented as shown in Fig. 2-5b, then during MISR operation,  $D_j = Q_i \oplus (Q_i p + Q_i' q) = Q_i p' + Q_i' q$ . Any error in  $p$  or  $q$  that is observable at  $Z_j$  (an error in  $p$  is observable when  $Q_i$  is 1; an error in  $q$  is observable when  $Q_i$  is 0) is also observable at  $D_j$  (i.e., captured in the MISR) during MISR operation. However, an error in  $Q_i$  is only observable at  $D_j$  (i.e., transferred to the next bistable in the MISR) when  $p = q$ , because when  $p = q = 0$ ,  $D_j = Q_i$ , and when  $p = q = 1$ ,  $D_j = Q_i'$ , whereas when  $p = q'$ ,  $D_j = 0$ . If the bistables in the scan path are arranged such that  $B_i$  precedes bistable  $B_k$  where  $Q_i$  is not essential for  $Z_k$ , then during MISR operation,  $D_k = Q_i \oplus Z_k$ , and all errors in either  $Q_i$  or  $Z_k$ , but not both, are observable at  $D_k$ . Therefore, case-4 scan dependence reduces the observability of errors in the previous bistable in the scan path, but does not reduce the observability of system logic errors.

The goal of our synthesis technique is to determine the arrangement of system bistables in an embedded MISR that has the maximum amount of beneficial scan dependence and no non-beneficial scan dependence (case-4 equations). The procedure first creates a directed graph called a *dependence graph*, where the nodes of the graph represent the system bistables. We add

a weighted edge from node  $i$  to node  $j$  if  $Z_j$  is a case-1, case-2, or case-3 function of  $Q_i$  (see Table 4-2). The weight of the edge represents the cost of the test logic overhead, either the performance overhead, the area overhead, or a combination of the two. We also add a weighted edge from node  $i$  to node  $j$  if  $Q_i$  is not essential for  $Z_j$ . In this case, bistable  $B_j$  is not scan dependent on  $B_i$ , and the weight of the edge represents the cost of the test logic overhead of Fig. 2-5b. No edge is added from node  $i$  to node  $j$  if  $Z_j$  is a case-4 function of  $Q_i$  since this represents a scan dependence situation that we wish to avoid. The best order of bistables is determined by finding the lowest-cost Hamiltonian cycle in the graph, where the cost of the cycle is the sum of the weights of the edges in the cycle. A Hamiltonian cycle contains all nodes in the graph, and all nodes in a Hamiltonian cycle are distinct. Frieze [Frieze 88] describes a polynomial-time algorithm for finding Hamiltonian cycles in directed graphs.

Unfortunately, some designs have a dependence graph that does not contain a Hamiltonian cycle. For example, if a system bistable is a case-4 function of all other bistables in the MISR, its corresponding node in the dependence graph has no incoming edges and can therefore not be included in a Hamiltonian cycle. We solve this problem by adding nodes to the graph, one at a time, until a Hamiltonian cycle is created. Adding a node to the dependence graph corresponds to adding a bistable to the design that is only used during test operations. Since the added bistable does not have a system logic function, it can perform a shift operation during both MISR mode and normal mode, so a case-1 edge is added from each node in the graph to the new node. Also, the output of the new bistable is not essential for any of the system bistable functions, so a “non-essential” edge is added from the new node to each “system” node in the graph. In the worst case, which corresponds to an original dependence graph with  $n$  nodes and no edges (each bistable is a case-4 function of every other bistable),  $n$  nodes must be added to create a Hamiltonian cycle, and the cycle will have alternating “system” and “test-only” nodes.

### 4.3 IMPLEMENTATION AND RESULTS

We have implemented both our synthesis technique (called *BSD* for *beneficial scan dependence*) and the synthesis technique of avoiding all types of scan dependence (called *AVD*) using procedures from the *SIS* logic synthesis tool [Sentovich 92]. The synthesis techniques use the categories listed in Table 4-2 to first identify the different dependence cases for each bistable input and create a dependence graph. Then, for the *BSD* technique, the bistables are arranged into a circular BIST scan path that has the maximum number of case-1, case-2, and case-3 functions, and no case-4 functions. For the *AVD* technique, the bistables are arranged into a circular BIST scan path that has no scan dependencies. For both techniques, “test-only” vertices are added one at a time to the dependence graph, if necessary, until a Hamiltonian cycle is created. We applied the synthesis techniques to the ACM/SIGDA LGSynth91 benchmark

circuits [ACM 91] and provide both implementation results and fault simulation results in this section.

Table 4-3 lists the number of system and test-only bistables in the generated circular BIST versions of the benchmark circuits, and the number of beneficial scan dependence equations in the *BSD* versions of the benchmark circuits. Twelve of the 23 benchmark circuits have no instances of beneficial scan dependence in the circular BIST path selected by the *BSD* technique, so there is no difference between the *AVD* and *BSD* versions of these circuits. Additional implementation details of the remaining circuits, highlighted in Table 4-3, are provided in Tables 4-4, 4-5, and 4-6.

#### 4.3.1 Area and Delay Results

Tables 4-4 and 4-5 compare area and delay values for the circular BIST benchmark circuits. For both tables, the *SIS* logic synthesis tool [Sentovich 92] was used to apply multi-level logic optimizations, and the *CERES* technology mapping tool [Mailhot 93] was used to map the logic to LSI logic 1.0 micron standard cell gates [LSI 91]. The area values are given in terms of LSI logic cell units, and the delay values are in nanoseconds. “% Overhead” is the percentage increase in area or delay of the circular BIST version of the circuit over the system logic version with no test logic added. “% Diff” is the percentage decrease in area or delay of the *BSD* version of the circuit over the *AVD* version. Area optimization techniques were used for both logic optimization and technology mapping for the circuits in Table 4-4, and delay optimization techniques were used for the circuits in Table 4-5.

**Table 4-3** Bistable characteristics for circular BIST benchmark circuits.

Circuit	AVD Bistables		BSD Bistables		# BSD Eqns
	System	Test-Only	System	Test-Only	
s1196	18	0	18	0	0
s1488	6	6	6	6	0
s1494	6	6	6	6	0
s208.1	8	1	8	1	0
<b>s298</b>	<b>14</b>	<b>0</b>	<b>14</b>	<b>0</b>	<b>1</b>
s344	15	3	15	3	0
s349	15	3	15	3	0
<b>s382</b>	<b>21</b>	<b>0</b>	<b>21</b>	<b>0</b>	<b>3</b>
<b>s386</b>	<b>6</b>	<b>6</b>	<b>6</b>	<b>3</b>	<b>3</b>
<b>s400</b>	<b>21</b>	<b>0</b>	<b>21</b>	<b>0</b>	<b>3</b>
s420.1	16	1	16	1	0
<b>s444</b>	<b>21</b>	<b>0</b>	<b>21</b>	<b>0</b>	<b>3</b>
s510	6	6	6	6	0
<b>s526</b>	<b>21</b>	<b>0</b>	<b>21</b>	<b>0</b>	<b>1</b>
<b>s641</b>	<b>17</b>	<b>0</b>	<b>17</b>	<b>0</b>	<b>6</b>
<b>s713</b>	<b>17</b>	<b>0</b>	<b>17</b>	<b>0</b>	<b>8</b>
s820	5	5	5	5	0
s832	5	5	5	5	0
s838.1	32	1	32	1	0
<b>sbc</b>	<b>27</b>	<b>0</b>	<b>27</b>	<b>0</b>	<b>6</b>
mm4a	12	0	12	0	0
<b>mult16b</b>	<b>30</b>	<b>0</b>	<b>30</b>	<b>0</b>	<b>14</b>
<b>mult32b</b>	<b>62</b>	<b>0</b>	<b>62</b>	<b>0</b>	<b>30</b>

**Table 4-4** Area and overhead for area-optimized circular BIST benchmark circuits.

Circuit	AVD		BSD		% Diff
	Area	% Overhead	Area	% Overhead	
s298	779	38.4	778	38.2	0.1
s382	1131	40.3	1110	37.7	1.9
s386	649	51.3	624	50.7	3.9
s400	1124	39.3	1111	37.7	1.2
s444	1137	44.3	1134	43.9	0.3
s526	1207	36.5	1206	36.4	0.1
s641	1534	42.6	1635	52.0	-6.6
s713	1539	43.4	1595	49.5	-3.6
sbc	3053	23.7	3045	23.4	0.3
mult16b	1516	46.7	1303	17.3	14.1
mult32b	3096	49.2	2648	16.5	14.5

**Table 4-5** Delay and overhead for delay-optimized circular BIST benchmark circuits.

Circuit	AVD		BSD		% Diff
	Delay	% Overhead	Delay	% Overhead	
s298	6.8	19.0	6.8	20.2	0.0
s382	7.3	33.6	7.4	36.3	-2.1
s386	6.8	20.0	7.9	39.1	-15.9
s400	6.8	26.7	6.8	26.7	0.0
s444	7.5	25.8	7.1	19.5	5.0
s526	6.7	11.4	6.8	12.9	-1.3
s641	11.7	31.9	11.5	29.4	1.9
s713	11.0	24.8	11.0	24.7	0.1
sbc	11.8	10.1	11.8	10.0	0.1
mult16b	9.1	-0.4	8.6	-6.6	6.1
mult32b	14.2	-13.1	13.7	-16.1	3.5

Table 4-6 shows the gate area overhead, net area overhead, and total area overhead for layouts of the circular BIST benchmark circuits. The layouts were generated using *SIS* for area-optimized logic optimization, *CERES* for area-optimized technology mapping, and *TimberWolf 6.0* for standard cell place and route. The circuits were mapped to version 2.2 of the scalable CMOS standard cell library that is included with the *TimberWolf* tool. We used the best of five different layouts generated by *TimberWolf* for each circuit in Table 4-6.

**Table 4-6** Layout area overhead for area-optimized circular BIST benchmark circuits.

Circuit	AVD % Overhead			BSD % Overhead			% Difference		
	Gate	Net	Total	Gate	Net	Total	Gate	Net	Total
s298	46.7	61.5	55.1	45.1	53.5	51.8	1.1	4.9	2.1
s382	44.8	62.4	53.7	44.3	62.3	53.7	0.4	0.1	0.0
s386	39.8	32.9	36.3	39.0	39.1	39.9	0.6	-4.7	-2.6
s400	45.1	51.5	49.7	43.8	55.7	52.9	0.9	-2.8	-2.1
s444	51.2	62.0	52.5	51.4	54.9	53.0	-0.1	4.3	-0.3
s526	39.5	53.5	49.3	38.3	53.8	49.3	0.9	-0.2	0.0
s641	45.1	57.0	54.3	55.3	71.9	68.2	-7.0	-9.5	-9.0
s713	44.4	56.5	53.9	53.9	68.5	67.3	-6.6	-7.6	-8.7
sbc	21.3	22.3	26.4	21.1	22.8	26.2	0.2	-0.4	0.2
mult16b	56.8	68.1	57.3	17.0	18.7	16.9	25.4	29.4	25.7
mult32b	57.3	84.5	74.5	16.1	15.2	14.6	26.2	37.6	34.3

For most of the benchmark circuits we investigated, the sizes of the *AVD* and *BSD* versions are not significantly different. Two of the *BSD* circuits (*s641* and *s713*) are larger than the *AVD* circuits. We determined that this is due to high fanout of some of the system logic equations that

are re-structured for beneficial scan dependence in the circular BIST path according to Fig. 4-4. An enhancement to the synthesis technique should consider the fanout of the system logic when determining whether or not a particular system logic equation is beneficial for scan dependence. According to Tables 4-4, 4-5, and 4-6, the *BSD* versions of two of the circuits (*mult16b*, *mult32b*) have significantly less area and delay than the *AVD* versions of these circuits. The reason for this low overhead is that both *mult16b* and *mult32b* perform a serial multiplication operation which has the property that many of the system logic equations are case-3 equations. Our synthesis technique is able to arrange the bistables into a circular BIST path such that most of the bistables are case-3 scan dependent on the previous bistable in the path, and these case-3 equations have very little overhead for BIST (see Fig. 4-4c). We focus on this property of arithmetic operations in the Sec. 5 discussion of scan dependence in data path logic.

### 4.3.2 Fault Simulation Results

We performed extensive fault simulations on several of the benchmark circuits in order to evaluate how scan dependence affects the quality of BIST operation. For each benchmark circuit, we created four different circuit models for gate-level, single stuck-at fault simulation: *FNL*, *IGN*, *AVD*, and *BSD*. The *FNL* version is the original benchmark circuit, and it executes normal operation during the fault simulation. The front-end test logic shown in Fig. 2-5b was used for every bistable in the *IGN* version (*IGN* stands for *ignore* scan dependence), and the bistables were arranged into a circular BIST path such that the number of scan dependent bistables was maximized. The *AVD* and *BSD* circuits were generated as described previously in this section. The fault simulation results are given in Table 4-7. The fault coverage is the percentage of collapsed, single stuck-at faults that are detected at least once during BIST operation, and is a measure of the quality of the TPG operation. We define *error loss* as the percentage of clock cycles for which the faulty and fault-free machines are identical (i.e., the percentage of aliased clock cycles) given that the fault has been detected. Error loss is a measure of the quality of the ORA operation. Table 4-7 shows that the *BSD* versions of the benchmark circuits have the highest fault coverage, and for most of the circuits, the lowest error loss. The slightly elevated error loss for the *BSD* version of circuit *s386* could be attributed to the fact that its circular BIST path has three fewer bistables than the *AVD* version. Even if a circuit has a high fault coverage percentage, a non-zero error loss percentage means that there is a chance that a defective circuit will be labeled fault-free even if the fault is detected at some time during the BIST operation. The defective circuit can only be identified if the BIST operation terminates on a non-aliased state.

**Table 4-7** Fault simulation results for circular BIST benchmark circuits.

Circuit	% Fault Coverage				% Error Loss			
	FNL	IGN	AVD	BSD	FNL	IGN	AVD	BSD
s298	33.3	100.0	100.0	100.0	49.1	0.6	0.2	0.0
s386	37.6	30.2	77.8	80.2	59.2	0.2	0.0	2.8
s444	35.5	100.0	100.0	100.0	50.5	0.0	0.0	0.0
s641	88.9	100.0	100.0	100.0	73.4	9.5	0.0	0.0
mult16b	100.0	98.6	100.0	100.0	37.9	26.0	0.0	0.0
mult32b	99.0	95.7	100.0	100.0	1.9	39.7	0.0	0.0

#### 4.4 CONTRIBUTIONS

In this section, we have given a formal definition for scan dependence and have shown that certain types of scan dependence, called beneficial scan dependence, can be used to reduce the area and delay of embedded BIST techniques. We have developed new ORA functions for these beneficial scan dependence equations. We have developed and implemented a new synthesis technique that, given a design described in terms of Boolean equations and bistables, creates a scan path that has the maximum amount of beneficial scan dependence and no non-beneficial scan dependence, and generates a circular BIST implementation of the design. Most of the circular BIST benchmark circuits generated by our synthesis technique are comparable in size and delay to circuits generated by other techniques. However, our results are significantly better for the two arithmetic circuits in the benchmark suite.

Finally, we have analyzed the effect that ignoring scan dependence has on fault observability during BIST operation. Fault simulations of circular BIST benchmark circuits confirms our analysis: ignoring scan dependence can increase the aliasing of the ORA function of circular BIST architectures. Our fault simulations have also shown that although fault coverage can be high for both normal operation and for BIST operation where scan dependence is ignored, the high error loss of the ORA function reduces the overall quality of the BIST operation for these circuits.

## 5 SCAN DEPENDENCE IN DATA PATH LOGIC

The synthesis technique described in Sec. 4 is a general technique for maximizing beneficial scan dependence given that the system logic is described in terms of Boolean equations and bistables. One way to maximize beneficial scan dependence in data path logic is to first apply high-level synthesis operations to a data flow description of the design, then apply the technique described in Sec. 4 to the generated data path logic. Unfortunately, due to the types of function blocks typically found in data path logic (e.g., multipliers, adders), generating the dependence graph for the data path bistables could be very computationally expensive. More importantly, the high-level synthesis technique may generate data path logic with few beneficial dependencies between the bistables.

In this section, we describe a method for increasing the beneficial dependencies between system bistables during high-level synthesis. There are several advantages when beneficial scan dependence is considered during high-level synthesis of data path logic, where the input to synthesis is a data flow description, rather than Boolean equations. First, we can simplify the generation of the dependence graph since the Boolean equations for the system logic can be inferred for multiple bistables given a single operation in a data flow equation. For example, given the data flow equation  $R3 = R1 \text{ ADD } R2$ , where  $R1$ ,  $R2$ , and  $R3$  are  $n$ -bit registers, we can infer that the system logic equation for each bistable,  $B_i$ , of register  $R3$  has the form  $R3_i = R1_i \oplus R2_i \oplus C_i$ , where  $C_i$  is the carry function for  $B_i$ . We need not perform Shannon decomposition on the system logic equations of the addition operation in order to determine the dependence information for the bistables in  $R3$ . Second, in data path logic, all bistables in a register are typically controlled by the same group of control signals. When test operation control signals can be used in the same manner, i.e., one block of test control logic for each register rather than for each bistable in the design, test overhead can be reduced. Finally, since the synthesis technique determines how variables in the data flow description are assigned to bistables, it may be able to generate data path logic with more instances of case-1, case-2, and case-3 dependencies between the bistables, resulting in a lower-cost, self-testable design.

This section is a summary of the material in [Avra 92] and Sec. 6 of [Avra 94a] and contains a discussion of how to apply the synthesis technique described in Sec. 4 to data path logic. We first describe a new scan path architecture for data path logic, called *orthogonal scan path*, where the shift direction in the orthogonal scan path is orthogonal to the shift direction in traditional scan paths (shifting bits within registers). We then identify data path functions that are well-suited for the synthesis technique described in Sec. 4, and show that the occurrence of these functions can be increased if an orthogonal scan path is used in the data path logic. Finally, we discuss a register binding technique that, assuming an orthogonal scan path architecture, attempts

to maximize the number of beneficial scan dependence equations in the generated data path logic.

### 5.1 ORTHOGONAL SCAN PATH ARCHITECTURE

Figure 5-1a is an example of logic that is commonly found in data path designs. The outputs of two registers,  $R1$  and  $R2$ , are the inputs to a combinational logic unit, *Adder*, that performs the addition operation, the output of which is stored in register  $R3$ . Each of the registers consists of  $n$  bistables. Traditional scan path architectures are arranged as shown in Fig. 5-1b, where each bistable of register  $R1$  feeds the next bistable of register  $R1$  during scan operation. When BIST is implemented in the data path logic, this scan path arrangement implies a correspondence between system registers and BIST registers, such as LFSRs and MISRs. For example, registers  $R1$  and  $R2$  could be implemented as LFSRs and  $R3$  could be implemented as a MISR during BIST operation if the parallel BIST architecture is used.

Figure 5-1c shows the bistable arrangement for an orthogonal scan path. Each bistable of  $R1$  feeds the corresponding bistable of register  $R3$  during scan operation. The outputs of  $R3$  may, in turn, be inputs to another register in the data path logic during scan operation. Note that, for this example, the flow of data during normal operation (from  $R1$  to  $R3$ ) is parallel to the flow of data during scan operation. This may allow for the sharing of system and test logic, which is the motivation for the orthogonal scan path arrangement.

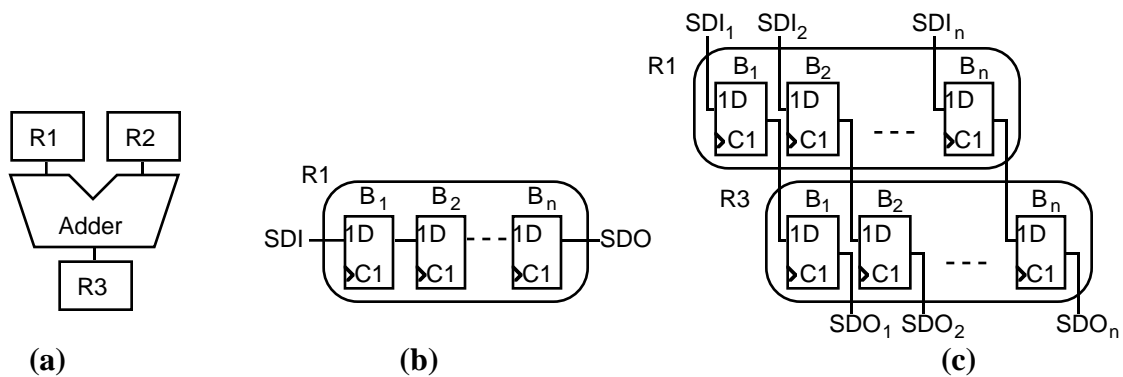


**Figure 5-1** Orthogonal scan path example: (a) normal operation; (b) typical scan path arrangement for  $R1$ ; (c) orthogonal scan path arrangement for  $R1$ .

### 5.2 SCAN DEPENDENCE FUNCTIONS IN DATA PATH LOGIC

The system logic equations for the bistables in register  $R3$  in Fig. 5-1a have the general form  $R3_i = R1_i \oplus R2_i \oplus C_i$ , where  $C_i$  is the carry function for bistable  $B_i$  of  $R3$ . Since  $C_i$  is a function of the less-significant bistables of  $R1$  and  $R2$ , and is not a function of  $R1_i$  or  $R2_i$ , each bistable in  $R3$  is a case-3 function of the corresponding bistable in  $R1$  and the corresponding bistable in  $R2$ . The implementation for case-3 equations shown in Fig. 4-4c can only be used if the bistables in

either  $R1$  or  $R2$  immediately precede the corresponding bistables in  $R3$  in the scan path. This can be accomplished when an orthogonal scan path is used in the data path logic.

Table 5-1 lists seven types of system logic equations for bistables in data path logic that we have determined can benefit from scan dependence. The equation type and an associated area overhead cost estimate based on LSI Logic cell units [LSI 91] are listed, where  $n$  represents the width of the data path (i.e., the number of bistables in each register). Lower-case letters  $a$  and  $b$  represent system logic control signals that determine the input to each bistable of register  $R1$ . Upper-case letters  $F$  and  $G$  represent outputs of combinational logic, the inputs to which are primary inputs and outputs of bistables excluding the corresponding bistables associated with register  $R2$ . For example, for a 2-bit data path ( $n = 2$ ), the equation  $R1 = a' R2 + a F$  represents two system logic equations:

$$\begin{aligned} ZI_0 &= a' Q2_0 + a F_0 \\ ZI_1 &= a' Q2_1 + a F_1 \end{aligned}$$

where  $F_0$  is not a function of  $Q2_0$ , and  $F_1$  is not a function of  $Q2_1$ .

**Table 5-1** System equations for data path registers that benefit from scan dependence.

Type	Cost	Function
1	0	$R1 = R2$
2	4	$R1 = a' R2 + a (R2 \oplus F)$
3	$4n$	$R1 = R2 \oplus F$
4	$12+2n$	$R1 = a' b' R2 + a' b (R2 \oplus F) + a G$
5	$4+8n$	$R1 = a' (R2 \oplus F) + a G$
6	$8+8n$	$R1 = a' R2 + a F$
7	$10n$	$R1 = R2 + F$
8	$18n$	$R1 = F$

Data flow equation types 1, 7, and 3 correspond to the case-1, case-2, and case-3 equations, respectively, described in Sec. 4.2, and the bistables of these registers can be implemented as shown in Fig. 4-4. Equation types 2, 4, 5, and 6 are combinations of case-1 and case-3 equations and have control logic can be shared between the test control signals and system control signals  $a$  and  $b$ . If the system logic equation for  $R1$  cannot be classified as one of the first seven types of equations shown in Table 5-1, it is classified as type 8, and the more general synthesis technique described in Sec. 4 can be applied to determine whether or not beneficial scan dependence exists for any of the bistables in the register. Register  $R3$  in Fig. 5-1a can be represented by the type-3 equation in Table 5-1,  $R1 = R2 \oplus F$ .

We have identified two types of operations that are common in data path designs and can be mapped to equation types 1-6 in Table 5-1: addition operations and live variable motion. Addition operations are common in DSP-based data path designs. [Waser 82] describes several

types of adder implementations, including conditional sum, Ling, and carry-look-ahead adders. The output equations for each of these adder implementations can be expressed as:  $RI_i = R2_i \oplus R3_i \oplus C_i$ , where  $C_i$  is a function of the less-significant bistables of  $R2$  and  $R3$ , and is not a function of  $R2_i$  or  $R3_i$ . The logic implementation for  $C_i$  varies with adder type. If any of the variables in the data flow description that are assigned to register  $R1$  are the result of an addition operation, it may be possible to implement  $R1$  by one of equation types 2-5 in Table 5-1.

Another type of function that can occur in data path designs is the transfer of data from one register to the next, known as *live variable motion*. Variables whose lifetimes are longer than one clock cycle can either be held in a single register, or transferred from one register to another. When the latter technique is used, equations of the form  $RI = a R2 + a' F$  occur in the data path logic, where a live variable is transferred from  $R2$  to  $R1$  whenever control signal  $a = 1$ . Depending on the logic that generates  $F$ , this equation can be mapped to equation types 1, 2, 4, 5, 6, or 7 in Table 5-1. Figure 5-2a is a data flow graph illustrating live variable motion. Variable  $H$  is loaded into register  $R3$  during the first clock cycle, but is not needed for computation until the second clock cycle, and so is loaded into  $R2$  during the second clock cycle. Variable  $G$  is loaded into  $R2$  during the first clock cycle. The system logic equations for the bistables of  $R2$  are type-6 equations, which can be implemented as shown in Fig. 5-2b. The control signal  $a$  is high during the first clock cycle and low during the second. The test logic overhead for this case consists of two AND gates per bistable in  $R2$  plus an AND gate and an OR gate to generate control signals for all bistables in the register. The exclusive-OR gate is used to perform the MISR function during BIST operation and a multiplexer function during normal operation.

### 5.3 RESULTS

Our high-level synthesis procedure for beneficial scan dependence assumes that the data path logic has an orthogonal scan path architecture, and biases the register binding operation to assign variables in the data flow equations to registers such that equation types 1-7 listed in Table 5-1 are used most often. This synthesis procedure was applied to two high-level synthesis benchmark circuits, *Tseng* [Tseng 86] and *DiffEq* [Paulin 89a]. The results are presented in Table 5-2. The size of the data path (in LSI Logic cell units [LSI 91]) and the overhead for test logic as a percentage of total size are given for two situations: 1) bistables are arranged into orthogonal scan paths after register binding (labeled “Test Synthesis”), and 2) equation types 1-7 in Table 5-1 are favored during register binding (labeled “Synthesis-for-Test”). We assumed a 16-bit data path, and estimated interconnect area as being one cell unit per interconnection. For both the test synthesis and synthesis-for-test procedures, beneficial scan dependence was maximized by using an orthogonal scan path arrangement in a circular BIST architecture. For

both examples, the total size and the test overhead are smaller when scan dependence is considered during register binding.

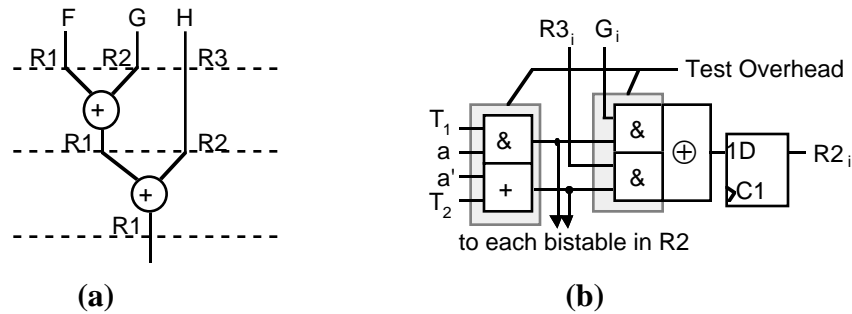


**Figure 5-2** Live variable motion: (a) data flow graph; (b) implementation of bistables in  $R2$ .

**Table 5-2** Data path design examples with orthogonal scan path and circular BIST.

Design	Test Synthesis		Synthesis-for-Test	
	Size (cell units)	% Overhead	Size (cell units)	% Overhead
Tseng	14,146	13.5	11,574	6.4
DiffEq	12,342	11.7	11,518	7.3

#### 5.4 CONTRIBUTIONS

We have developed a new scan path architecture for data path logic called orthogonal scan path. The motivation for using this type of scan path arrangement is that it can increase the number of beneficial dependencies between the bistables in the data path logic, which allows for more sharing of system and test logic. We have identified seven types of data path equations that are beneficial for scan dependence, and have shown that using an orthogonal scan path increases the occurrence of these types of equations. We discussed the synthesis of two data path design examples and showed that, when the register binding operation assumes an orthogonal scan path and is biased toward generating data path logic with certain structures for addition operations and live variable motion, lower-cost circular BIST designs result.

## 6 SYNTHESIS-FOR-TEST DESIGN SYSTEM

In this section, we describe a computer-aided design system, named Odin, that automatically generates a synchronous hardware design given a behavioral, VHDL description of the design. Existing hardware synthesis systems typically use cost and performance as the main criteria to be satisfied when generating a design from a behavioral description, and seldom even consider test issues during the synthesis process. The purpose of Odin is to serve as a platform for the development of synthesis techniques that generate low-cost, high-performance hardware implementations that also meet specified testability requirements. By considering testability during the synthesis process, Odin is able to generate designs that are optimized for specific test techniques. Odin can currently generate designs optimized for both parallel and circular BIST architectures.

We have implemented in Odin all of the major design system algorithms necessary for the generation of data path and control logic given a behavioral VHDL description: VHDL input and output file processing algorithms, internal data structure creation and manipulation algorithms, and high-level synthesis algorithms. Emphasis was placed on ease of modification when implementing the system in order to encourage the addition of future synthesis-for-test techniques. In this section, we describe the current capabilities of Odin. A more detailed description is given in [Avra 94b]. Section 6.1 is a brief overview of the Odin design system. Section 6.2 describes the VHDL input and output files for the design system: the input behavioral description, the component library that Odin accesses when performing synthesis operations, and the output structural description. Section 6.3 contains a description of the hierarchical data and control flow graph that is Odin's major internal data structure. Finally, in Sec. 6.4, we describe the high-level synthesis operations that are currently implemented in Odin.

### 6.1 OVERVIEW

Figure 6-1 illustrates the flow of tasks that are performed by the Odin design system. The input to Odin is a VHDL intermediate format (VIF) description that represents the behavioral description of the design. A commercial VHDL compiler, developed by Vantage Analysis Systems, is used to create VIF from the input behavioral description. Several transformations are applied to the VIF description in order to simplify Odin's internal data structures. VIF access routines supplied by Vantage are used to transform the VIF description into a data and control flow graph (DCFG). Compiler optimizations are applied to the DCFG in order to minimize the amount of code that must be mapped to hardware. If the behavioral VHDL description contains multiple process statements, inter-process communication can be analyzed [Martinolle 91] in order to extract all potential functional parallelism in the description so that the most efficient

hardware can be synthesized. The first task in high-level synthesis is scheduling, where operations (e.g., addition, comparison, multiplication) in the behavioral description are assigned to specific clock cycles based upon data dependencies and the delays of the hardware components that are used to implement the operations. Operations and variables are then mapped to hardware components from a user-specified VHDL component library. Control logic that generates control signals for the components in the data path logic is synthesized based upon the selected schedule and the binding of operations and variables to hardware components. The output is structural VHDL descriptions of control logic and data path logic that implement the input behavioral description.

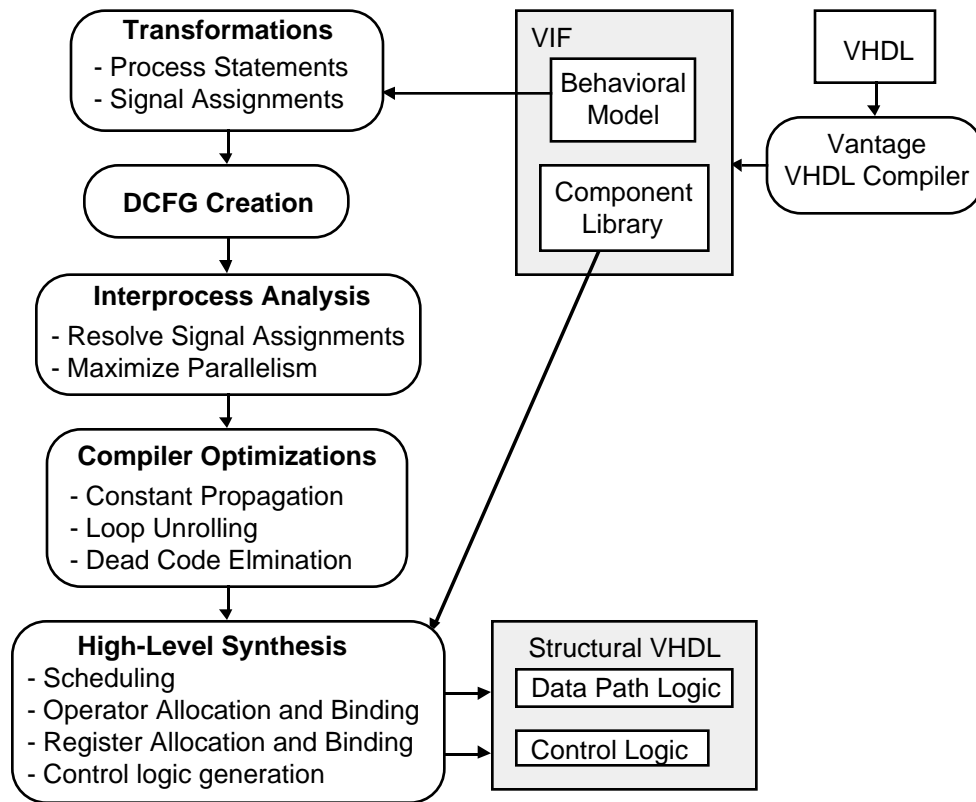


**Figure 6-1** Odin design system overview.

## 6.2 DESIGN SYSTEM INPUT AND OUTPUT

As shown in Fig. 6-1, the input to Odin consists of two VIF data structures, generated by the Vantage compiler from VHDL source code. The data structures represent a behavioral model of the design and a library of hardware components used by the synthesis techniques to generate a structural implementation.

### 6.2.1 VHDL Descriptions

The VHDL behavioral description of the design to be synthesized consists of algorithmic, high-level software constructs such as conditional statements, assignment statements, and loops. The behavioral description does not necessarily contain information, such as clock signal designations, that implies how it should be implemented in hardware. Table 6-1, a process statement from the *DiffEq* benchmark circuit description in [HLSW 92], is an example of the type of behavioral description that Odin accepts as input.

**Table 6-1** Example VHDL behavioral description: *DiffEq* from [HLSW 92].

---

```

process (Aport, DXport, Xinport, Yinport, Uinport)
  variable x_var,y_var,u_var, a_var, dx_var: integer ;
  variable x1, y1, t1,t2,t3,t4,t5,t6: integer ;
begin
  x_var := Xinport; y_var := Yinport; u_var := Uinport;
  a_var := Aport; dx_var := DXport;
  while (x_var < a_var) loop
    t1 := u_var * dx_var;
    t2 := 3 * x_var;
    t3 := 3 * y_var;
    t4 := t1 * t2;
    t5 := dx_var * t3;
    t6 := u_var - t4;
    u_var := t6 - t5;
    y1 := u_var * dx_var;
    y_var := y_var + y1;
    x_var := x_var + dx_var;
  end loop;
  Xoutport <= x_var;
  Youtport <= y_var;
  Uoutport <= u_var;
end process;

```

---

The VHDL structural descriptions of the control and data path logic generated by Odin are netlists that consist of component instantiations and signal interconnections. All components in the structural description are specified in the component library. A portion of an example VHDL structural description of data path logic generated by Odin is shown in Table 6-2. Three components (*ADD*, *SEL2*, and *SUB*) and their signal interconnections (*port map* statement) are shown. The *generic map(16)* statement specifies that the data path for that component is 16 bits, so, for example, the two data input signals, *INTERNAL14* and *INTERNAL9* for the *ADD* component are each 16 bits.

**Table 6-2** Example VHDL structural description of data path logic generated by Odin.

---

```

architecture STRUCTURAL of DATA_1 is
use work.COMPONENT_PKG.all;
.....
G14: ADD
  generic map(16)
  port map(INTERNAL8,INTERNAL14,INTERNAL9,cIn);
G15: SEL2
  generic map(16)
  port map(INTERNAL7,SEL(13),SEL(14),INTERNAL13,INTERNAL20);
G16: SUB
  generic map(16)
  port map(INTERNAL6,INTERNAL18,INTERNAL7,cIn);
.....
end STRUCTURAL;

```

---

### 6.2.2 Component Library

The VHDL structural description generated by Odin consists of hardware components that are specified by the user in a VHDL component library. Odin assumes that any operation in the behavioral description can be implemented by one or more components in the component library. The library must also contain register components and multiplexer or selector components for implementing the data path logic, and basic logic gates (e.g., NAND, NOR, INVERT) and bistables for implementing the control logic. The user is able to guide the synthesis process by means of the types of components available in the library and the characteristics associated with each available component. For example, by including in the library components that have been optimized for scan architectures, the user can minimize the overhead of any scan designs that Odin generates.

Associated with each component in the component library are attributes that specify its area, delay, and control information. The area attribute is used by Odin to estimate the cost of the component, and the delay attribute is used to estimate its performance. Since a single component may implement multiple operations (e.g., ALUs, comparators), the control information attributes specify the control signal values required for the component to implement the associated operation. Components that implement operations with multiple inputs also have an attribute that specifies whether or not the operation is commutative. The inputs to a commutative component can sometimes be switched to reduce the number of interconnections in the data path logic.

### 6.3 DATA AND CONTROL FLOW GRAPHS

The data and control flow graph (DCFG) is generated from the VHDL intermediate format and provides an accurate and concise means of conveying the information flow of the behavioral

description to the compiler optimization and synthesis operations. The DCFG has two levels of hierarchy. The top level is created by partitioning the behavioral description into basic blocks and control statements. A *basic block* is a sequence of consecutive assignment statements from the behavioral description. Figure 6-2a shows an example VHDL behavioral description that is partitioned into two control statements (circled), a *wait* and an *if*, and two basic blocks. The DCFG has six different types of nodes: *Wait*, *If*, and *Case*, which correspond to wait, if, and case statements, respectively, *While* for loop statements, *EndCond* for joining the mutually-exclusive branches of conditional statements, and *BB* for basic blocks. The information associated with each node depends upon its type. For example, *Wait* nodes are numbered since there are typically multiple wait statements in a VHDL behavioral description. Each *Wait* node also has a pointer to the list of signals to which the corresponding wait statement is sensitive. Figure 6-2b shows the top level of the DCFG for the process statement given in Fig. 6-2a. The five nodes are labeled  $N_1 - N_5$ . Edges in the DCFG represent the branching of operation between the behavioral statements represented by the nodes. A value associated with an edge represents the condition under which that branch is taken.

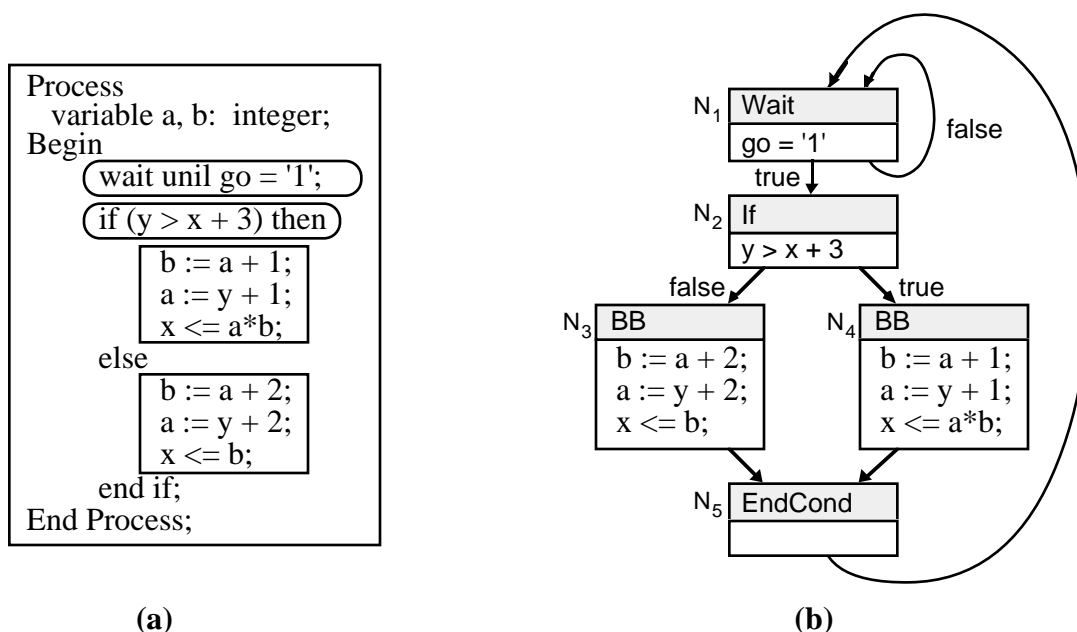


**Figure 6-2** DCFG example: (a) partitioned behavioral description; (b) top level of the DCFG.

A data flow graph (DFG) is associated with each node in the DCFG except for *EndCond* nodes. The data flow graph is a directed, acyclic graph that specifies the operations and the data dependencies of a basic block or an expression. Each node in the DFG represents an operation in the behavioral description. A directed edge from node  $N_i$  to node  $N_j$  specifies that the output of the operation represented by node  $N_i$  is an input to the operation represented by node  $N_j$ . Each

DFG has a source node (*SRC*) which only has outgoing edges that represent variables that are outputs of other DFGs, and a sink node (*SNK*) which only has incoming edges that represent variables that are inputs of other DFGs. The DFG for basic block nodes specifies how the variables defined by the statements in the basic block (a variable is *defined* if it appears on the left-hand-side of an assignment statement) are used in subsequent statements of the block (see Fig. 6-3a). The DFG for control nodes (*Wait*, *For*, *While*, *If*, *Case*) represents the conditional expression associated with the control statement. For example, the DFG associated with an *If* node represents the conditional expression of the *If* statement (see Fig. 6-3b).

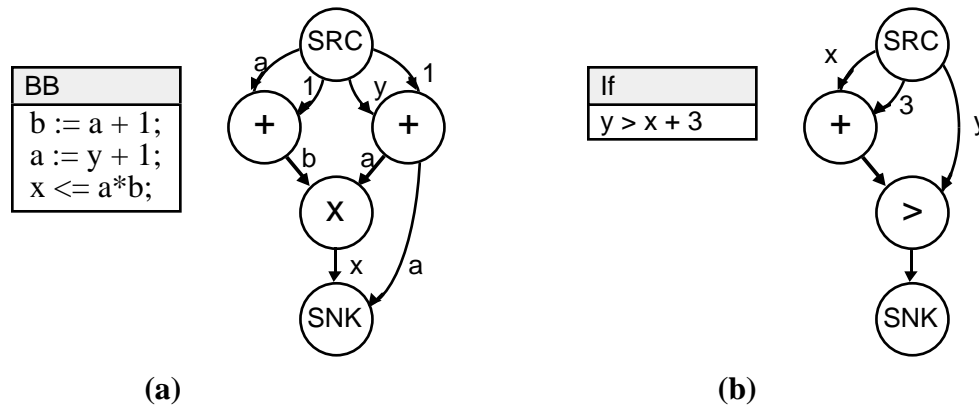


**Figure 6-3** Data flow graphs: (a) *BB* node DFG; (b) *If* node DFG.

Odin uses the DCFG to perform several basic compiler optimizations on the input behavioral description in order to minimize the amount of code that must be mapped to hardware and to improve the performance of the final design. The first optimization performed is constant propagation, where each use of a constant is replaced with its value. This simplifies expressions in the behavioral description and reduces the cost of the hardware that implements those expressions. For example, the expression  $x=y$  can be implemented in hardware with  $n$  exclusive-NOR gates and one  $n$ -input AND gate, where  $x$  is an  $n$ -bit variable, and  $y$  is an  $n$ -bit constant with value 17. When constant propagation is applied, the resulting expression,  $x=17$ , can be implemented with just one  $n$ -input AND gate. Next, Odin analyzes the flow of data in the DFGs in order to identify dead code (statements that can be removed without affecting the behavior of the description) that can be eliminated from the behavioral description. Since dead code does not contribute to the behavior of the design, Odin removes it before synthesis so that it is not mapped to hardware. Dead code may result from previously-applied compiler optimizations, such as constant propagation, or may be inadvertently introduced by the designer. The final optimization applied to the DCFG is to unroll loops with definite limits, where the limits do not exceed a specified maximum. The statements within a loop are executed sequentially for each iteration of the loop. When the data dependencies between the statements within the loop are such that they

can be executed in parallel, unrolling the loop reduces the number of clock cycles required to execute the loop statement.

#### 6.4 HIGH-LEVEL SYNTHESIS TECHNIQUES

An overview of the high-level synthesis tasks of scheduling, allocation, and binding is given in Sec. 3.1. In this section, we describe the high-level synthesis algorithms implemented in Odin.

The first high-level synthesis task that Odin performs is scheduling, where the operations in each DFG are assigned to execute in specific clock cycles. We have implemented Paulin's forced-directed scheduling algorithm [Paulin 89a] which attempts to minimize the area of the data path logic by evenly distributing the number of operations executed in each clock cycle without increasing the total number of clock cycles for the DFG. The scheduling algorithm uses the delay and area attributes of the components in the component library to perform this operation. After the schedule has been defined, operations in the DFG are bound to specific function blocks by a greedy algorithm that simply binds each operation in a clock cycle to the first available function block that performs that operation. For example, for the first clock cycle in Fig. 6-6a, Odin first binds one of the addition operations to the *ADD1* function block, then binds the second addition operation to the *ADD2* function block.

The register allocation and binding algorithms are implemented as described in Sec. 3, where the number of self-adjacent registers is minimized when a parallel BIST architecture is specified by the user. We have also implemented a register allocation and binding algorithm that allows self-adjacent registers in the data path logic, the only difference being that testability conflict edges are not added to the register conflict graph. Having both algorithms allows us to compare parallel BIST implementations with implementations that have been optimized without considering testability.

Odin generates multiplexers for the inputs of registers and function blocks in order to accommodate the flow of data required by the scheduled, bound DFG. Multiplexer generation for register inputs is performed in a straightforward manner by using the DFG to determine the source of data for each register at each clock cycle. For example, the register in Fig. 6-4a that receives input data from variable *c* in the first clock cycle receives input data from the output of *ADD2* in the second clock cycle and from the output of *ADD1* in the third clock cycle. This register therefore requires a 3-to-1 multiplexer on its input as shown in Figs 6-4b and 6-4c. Generation of multiplexers for function block inputs is performed in the same manner except that, when the operation is commutative, Odin attempts to reduce the size of the input multiplexers by permuting the function block inputs. For example, Fig. 6-4b shows that two, 3-to-1 multiplexers are required for the inputs to *ADD1* when the left and right inputs of the

addition operation in the DFG correspond to the left and right inputs of the function block in the data path logic. Since the addition operation is commutative, however, the left and right inputs to *ADD1* can be switched for one or more clock cycles. For this example, by switching the inputs for the second clock cycle, Odin generates two 2-to-1 multiplexers for the inputs of *ADD1* (Fig. 6-4c).

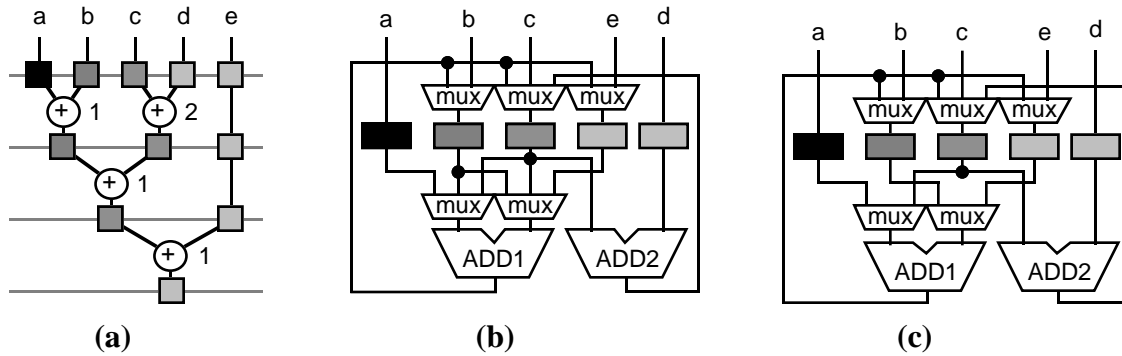


**Figure 6-4** High-level synthesis example: (a) scheduled, bound data flow graph; (b) data path logic; (c) data path logic with optimized multiplexers.

The last synthesis operation that Odin performs is to generate a control logic state machine that supplies register enable signals, multiplexer select signals, and function block control signals to the data path logic. Each block of data path logic corresponds to the DFG of a node in the DCFG and can be controlled by a mod- $m$  counter, where  $m$  is the total number of clock cycles for the scheduled DFG. The DFG counters are reset, enabled, and disabled by control logic that is generated from information in the DCFG edges. Odin combines all of the counters and the DCFG control logic into a single state machine. Figure 6-5 is a possible control logic state machine description for the process statement in Fig. 6-2, where  $N_{ij}$  represents clock cycle  $j$  of the scheduled DFG of DCFG node  $N_i$ . For example, DCFG node  $N_2$  in Fig. 6-2b represents the *if* statement in Fig. 6-2a. Assume that the output of the *if* statement conditional expression,  $y > x+3$ , is generated in two clock cycles in data path logic. Then, when the control logic state machine in Fig. 6-5 is in state  $N2_1$ , the first clock cycle of the DFG for  $y > x+3$  is executed, and when the machine is in state  $N2_2$ , the second clock cycle is executed. Odin generates a *KISS* format description of the control logic state machine, then uses procedures from the *SIS* logic synthesis tool [Sentovich 92] to perform state assignment and logic optimization, and to generate a circular BIST state machine implementation as described in Sec. 4.

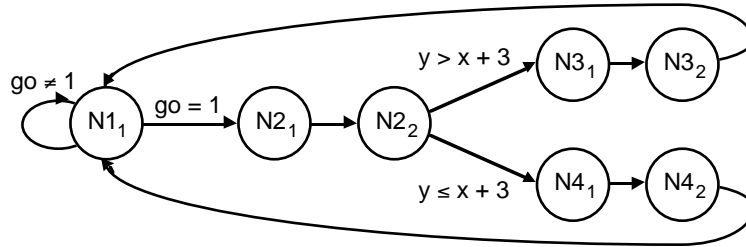


**Figure 6-5** Control logic state machine description for Fig. 6-2.

## 7 CONCLUDING REMARKS

In this dissertation, we have described new synthesis techniques that generate built-in self-testable designs. The primary objective of these *synthesis-for-BIST* techniques is to satisfy requirements associated with a specific BIST architecture when generating the system logic structural implementation. Cost is minimized and performance is maximized to the extent that BIST requirements are not compromised. Considering BIST issues during system logic synthesis allows for the generation of system logic that is optimized for a particular BIST architecture and that can be more effectively tested by the BIST operation.

In particular, we investigated techniques for generating low-cost, built-in self-testable designs that are free of the types of system bistable dependencies that can reduce the effectiveness of the embedded MISRs that are used to perform BIST operations. We showed that some types of system bistable dependencies can reduce the effectiveness of BIST, whereas other types of dependencies can allow sharing of BIST and scan logic with system logic, thereby reducing BIST overhead. Care must be taken, however, when system logic and BIST logic is shared, so that the BIST operation effectiveness is not compromised.

Our first synthesis technique, allocation and binding for parallel BIST (Sec. 3), minimizes the number of self-adjacent registers in the generated design without increasing the latency of the design. We have implemented the technique in our synthesis-for test design tool, and results show that, for the examples investigated, our technique generates the lowest-cost parallel BIST implementation and generates system logic that is comparable in cost to techniques that do not consider BIST during synthesis. There is one situation for which the generation of a self-adjacent register is unavoidable without changing the schedule or operation binding of the input data flow description. For this case, we use a CBILBO register, which breaks the self-adjacency during BIST operation. CBILBOs have a higher cost than regular BILBO registers, but have the advantage that they simultaneously perform the TPG and ORA operations. This can allow for a reduction in the number of test sessions required for BIST operation. The scheduling and operation binding techniques could be modified in order to minimize the number of unavoidable self-adjacencies encountered during register binding, and this is the subject of further research.

In Sec. 2, we showed that generating an ideal parallel BIST architecture requires addressing complex implementation details such as TPG interconnections, multiple feedback logic blocks, and test session scheduling. The synthesis technique described in Sec. 3 addresses only one of these implementation details: self-adjacent registers. One advantage of the ideal parallel BIST architecture is that the assumptions made in the generation of theoretical results for TPG fault coverage [Kim 88] and ORA aliasing [Daehn 90] characteristics are applicable, and these results can be used to estimate the test transparency of the BIST operation. Unfortunately, the

remaining implementation complexities must be addressed by synthesis techniques before automatic generation of an ideal parallel BIST architecture is feasible. It may be necessary for these techniques to consider more general system bistable (rather than system register) dependencies during high-level synthesis.

The synthesis techniques described in Secs. 4 and 5 address the more general problem of system bistable dependency during logic synthesis (Sec. 4) and high-level synthesis (Sec. 5). Both techniques attempt to maximize sharing of system logic and test logic to reduce the cost and improve the performance without increasing the test transparency of BIST architectures, such as circular BIST and parallel BIST, that make use of embedded MISRs. We have implemented the logic synthesis technique described in Sec. 4 in our system design tool and used it to generate circular BIST implementations of several sequential logic synthesis benchmark circuits. For most of the benchmark circuits we investigated, the sizes of the circuits generated by our technique did not differ significantly from the sizes of circuits with no scan dependence. However, better results for our technique should be possible when higher-level synthesis operations, such as state assignment and register binding, are biased toward generating more system bistables with beneficial dependence equations. Results presented in Sec. 5 showed that this is true for the register binding operation when an orthogonal scan path configuration is used. The orthogonal scan path allows for greater sharing of BIST logic and commonly-used data path logic such as multiplexers and adders.

While the synthesis technique described in Sec. 4 is applicable to any BIST architecture that uses embedded MISRs, our implementation of the technique generates circular BIST designs because circular BIST has far fewer complex implementation issues than the parallel BIST architecture. Unfortunately, theoretical results for TPG fault coverage and ORA aliasing are not valid for circular BIST because of the dependence of the MISR inputs on the state of the MISR. Extensive fault simulations of the circular BIST implementation must therefore be executed to guarantee high-quality BIST operation. Fault simulations of the designs generated by our synthesis technique show that the test transparency is comparable to circular BIST architectures that allow no scan dependence. These simulations also showed that for two common design practices, not including any BIST circuitry, or if circular BIST is implemented, ignoring scan dependence, fault coverage can be high, but high error loss reduces the overall quality of the BIST operation. This suggests that further investigation into techniques for improving the ORA characteristics of self-adjacent MISRs could yield lower-cost, self-testable designs.

## REFERENCES

- [Abadir 85] Abadir, M. S., and M. A. Breuer, "A Knowledge-Based System for Designing Testable VLSI Chips," *IEEE Des. and Test of Comput.*, pp. 56-68, August 1985.
- [Abramovici 90] Abramovici, M., M. A. Breuer, and A. D. Friedman, *Digital Systems Testing and Testable Design*, Computer Science Press, New York, NY, USA 1990.
- [ACM 91] ACM/SIGDA 1991 Logic Synthesis Benchmark Circuits, available via anonymous ftp from mcnc.mcnc.org.
- [Avra 90] Avra, L., and E. J. McCluskey, "Behavioral Synthesis of Testable Systems with VHDL," *Dig. COMPCON Spring 90*, San Francisco, pp. 410-415, February 26-March 2, 1990.
- [Avra 91] Avra, L., "Allocation and Assignment in High-Level Synthesis for Self-Testable Data Paths," *Int. Test Conf.*, Nashville, TN, USA, pp. 463-472, October 26-30, 1991.
- [Avra 92] Avra, L., "Orthogonal Built-In Self-Test," *COMPCON Spring 1992 Dig. of Papers*, San Francisco, CA, USA, pp. 452-457, February 24-28, 1992.
- [Avra 93] Avra, L. J., and E. J. McCluskey, "Synthesizing for Scan Dependence in Built-In Self-Testable Designs," *Int. Test Conf.*, Baltimore, MD, USA, pp. 734-743, October 17-21, 1993.
- [Avra 94a] Avra, L. J., and E. J. McCluskey, "Synthesizing for Scan Dependence in Built-In Self-Testable Designs," *Center for Reliable Comput. Tech. Rpt. 94-2*, Comput. Sys. Lab., CSL TR 94-621, Stanford University, Stanford, CA, May 1994.
- [Avra 94b] Avra, L. J., L. Gerboux, J.-C. Giomi, F. Martinolle, and E. J. McCluskey, "A Synthesis-for-Test Design System," *Center for Reliable Comput. Tech. Rpt. 94-3*, Comput. Sys. Lab., CSL TR 94-622, Stanford University, Stanford, CA, May 1994.
- [Bardell 82] Bardell, P. H., and W. H. McAnney, "Self-Testing of Multichip Logic Modules," *Int. Test Conf.*, pp. 200-204, November 1982.
- [Bardell 87] Bardell, P. H., W. H. McAnney, and J. Savir, *Built-In Test for VLSI: Pseudorandom Techniques*, John Wiley & Sons, Inc., 1987.
- [Bardell 91] Bardell, P. H., and M. J. Lapointe, "Production Experience with Built-In Self-Test in the IBM ES/9000 System," *Int. Test Conf. Proc.*, Nashville, TN, USA, pp. 28-36, October 26-30, 1991.
- [Bhatia 93] Bhatia, S. and N. K. Jha, "Synthesis of Sequential Circuits for Robust Path Delay Fault Testability," *6th Int. Conf. on VLSI Des.*, pp. 275-280, January 1993.
- [Bonnenberg 93] Bonnenberg, H, A. Curiger, N. Felber, H. Kaeslin, R. Zimmermann, and W. Fichtner, "VINCI: Secure Test of a VLSI High-Speed Encryption System," *Int. Test Conf.*, Baltimore, MD, USA, pp. 782-790, October 17-21, 1993.

- [Brayton 87] Brayton, R. K., R. Rudell, A. Sangiovanni-Vincentelli, and A. R. Wang, "MIS: A Multiple-Level Logic Optimization System," *IEEE Trans. on Comput.-Aided Des.*, Vol. CAD-6, No. 6, pp. 1062-1081, November 1987.
- [Broseghini 93] Broseghini, J., and D. H. Lenhert, "An ALU-Based Programmable MISR/Pseudorandom Generator for a MC68HC11 Family Self-Test," *Int. Test Conf.*, Baltimore, MD, USA, pp. 349-358, October 17-21, 1993.
- [Bryan 89] Bryan, D., F. Brglez, and R. Lisanke, "Redundancy Identification and Removal," *Int. Workshop on Logic Synthesis*, Research Triangle Park, NC, May 23-26, 1989.
- [Cheng 89] Cheng, K. T., and V. D. Agrawal, "An Economical Scan Design for Sequential Logic Test Generation," *Int. Symp. Fault-Tolerant Comput.*, Chicago, IL, USA, pp. 28-35, June 21-23, 1989.
- [Daehn 90] Daehn, W., T. W. Williams, and K. D. Wagner, "Aliasing Errors in Linear Automata Used as Multiple-Input Signature Analyzers," *IBM J. Res. Develop.*, Vol. 34, No. 2/3, pp. 363-380, March/May 1990.
- [De Micheli 94] De Micheli, Giovanni, "Synthesis and Optimization of Digital Circuits," McGraw-Hill, Inc., Hightstown, NJ, USA, 1994.
- [Devadas 90] Devadas, S., and K. Keutzer, "Synthesis and Optimization Procedures for Robustly Delay-Fault Testable Combinational Logic Circuits," *27th Des. Autom. Conf.*, Orlando, FL, pp. 221-227, June 24-29, 1990.
- [Frieze 88] Frieze, A. M., "An Algorithm for Finding Hamiltonian Cycles in Random Directed Graphs," *J. of Algorithms*, pp. 181-204, June 1988.
- [Gage 93] Gage, R., "Structured CBIST in ASICs," *Int. Test Conf.*, Baltimore, MD, USA, pp. 332-338, October 17-21, 1993.
- [Gelsinger 86] Gelsinger, P. P., "Built In Self Test of the 80386," *Int. Conf. Comput. Des.*, pp. 169-173, 1986.
- [Gupta 91] Gupta, R., and M. A. Breuer, "Ordering Storage Elements in a Single Scan Chain," *IEEE Int. Conf. Comput.-Aided Des.*, Santa Clara, CA, USA, pp. 408-411, November 11-14, 1991.
- [Hachtel 89] Hachtel, G. D., R. Jacoby, K. Keutzer, and C. Morrison, "On the Relationship Between Area Optimization and Multifault Testability of Multilevel Logic," *Int. Workshop on Logic Synthesis*, Research Triangle Park, NC, May 23-26, 1989.
- [Hao 91] Hao, H., and E. J. McCluskey, "'Resistive Shorts' Within CMOS Gates," *Int. Test Conf.*, Nashville, TN, USA, pp. 292-301, October 26-30, 1991.
- [HLSW 92] 1992 High-Level Synthesis Workshop Benchmark Circuits, available via anonymous ftp from [mcnc.mcnc.org](http://mcnc.mcnc.org).

- [Hudson 87] Hudson, C. L. Jr., and G. D. Peterson, "Parallel Self-Test with Pseudo-Random Test Patterns," *Dig. Int. Test Conf.*, Washington, DC, USA, pp. 954-963, September 1-3, 1987.
- [IEEE 88] IEEE Standard 1076-1987, "IEEE Standard VHDL Language Reference Manual," IEEE Standards Board, 345 East 47th Street, New York, NY 10017, 1988.
- [IEEE 90] IEEE Standard 1149.1-1990, "IEEE Standard Test Access Port and Boundary Scan Architecture," Institute of Electrical and Electronics Engineers, Inc., New York, NY, USA, 1990.
- [Illman 91] Illman, R., T. Bird, G. Catlow, S. Clarke, L. Theobald, and G. Willetts, "Built-In Self-Test of the VLSI Content Addressable Filestore," *Int. Test Conf. Proc.*, Nashville, TN, USA, pp. 37-46, October 26-30, 1991.
- [Jha 92] Jha, N.H., I. Pomeranz, S.M. Reddy, and R. Miller, "Synthesis of Multi-Level Combinational Circuits for Complete Robust Path Delay Fault Testability," *Int. Symp. on Fault-Tolerant Comput.*, Boston, MA, USA, pp. 280-287, July 8-10, 1992.
- [Kim 88] Kim, K. D. S. Ha, and J. G. Tront, "On Using Signature Registers as Pseudorandom Pattern Generators in Built-in Self-Testing," *IEEE Trans. on Comput.-Aided Des.*, Vol. 7, No. 8, pp. 919-928, August 1988.
- [Konemann 79] Konemann, B., J. Mucha, and G. Zwiehoff, "Built-In Logic Block Observation Techniques," *1979 IEEE Test Conf.*, Cherry Hill, NJ, USA, pp. 37-41, 1979.
- [Konemann 80] Konemann, B., J. Mucha, and G. Zwiehoff, "Built-In Test for Complex Digital Integrated Circuits," *IEEE J. of Solid-State Circuits*, Vol. SC-15, No. 3, pp. 315-319, June 1980.
- [Krasniewski 85] Krasniewski, A., and A. Albicki, "Automatic Design of Exhaustively Self-Testing Chips with BILBO Modules," *Int. Test Conf.*, Philadelphia, PA, USA, pp. 362-370, November 19-21, 1985.
- [Krasniewski 89] Krasniewski, A., and S. Pilarski, "Circular Self-Test Path: A Low-Cost BIST Technique for VLSI Circuits," *IEEE Trans. on Comput.-Aided Des.*, Vol. 8, No. 1, pp. 46-55, January 1989.
- [Lake 86] Lake, R., "A Fast 20K Gate Array with On-Chip Test System," *VLSI Systems Design*, pp. 46-55, June 1986.
- [Langford 93] Langford, T., "Utilizing Boundary Scan to Implement BIST," *Int. Test Conf.*, Baltimore, MD, USA, pp. 167-173, October 17-21, 1993.
- [Lee 93] Lee, T.-C., N. K. Jha, and W. H. Wolf, "A Conditional Resource Sharing Method for Behavioral Synthesis of Highly Testable Data Paths," *Int. Test Conf.*, Baltimore, MD, USA, pp. 744-753, October 17-21, 1993.
- [LSI 91] *LSI Logic 1.0-Micron Cell-Based Products Databook*, LCB007 Cell-Based ASICs, February 1991.

- [Mailhot 93] Mailhot, F., and G. De Micheli, "Algorithms for Technology Mapping Based on Binary Decision Diagrams and on Boolean Operations," *IEEE Trans. on Comput.-Aided Des.*, Vol. 12, No. 5, pp. 599-620, May 1993.
- [Martinolle 91] Martinolle, F., "Fusion of VHDL Processes," *Center for Reliable Computing Technical Report 91-7*, CSL-TN-91-384, Computer Systems Laboratory, Stanford University, Stanford, CA, USA, December 1991.
- [McCluskey 81] McCluskey, E. J., and S. Bozorgui-Nesbat, "Design for Autonomous Test," *IEEE Trans. on Comput.*, Vol. C-30, No. 11, pp. 866-874, November 1981.
- [McCluskey 85] McCluskey, E. J., "Built-In Self-Test Structures," *IEEE Des. and Test*, pp. 29-36, April 1985.
- [McCluskey 86] McCluskey, E. J., *Logic Design Principles with Emphasis on Testable Semicustom Circuits*, Prentice-Hall, Englewood Cliffs, NJ, USA, 1986.
- [McCluskey 88] McCluskey, E. J., S. Makar, S. Mourad, and K. D. Wagner, "Probability Models for Pseudo-Random Test Sequences," *IEEE Trans. on Comput.-Aided Des.*, Vol. 7, No. 1, pp. 68-74, January 1988.
- [McFarland 88] McFarland, M. C., A. C. Parker, and R. Camposano, "Tutorial on High-Level Synthesis," *25th ACM/IEEE Des. Autom. Conf.*, Anaheim, CA, USA, pp. 330-336, June 12-15, 1988.
- [Mujumdar 92] Mujumdar, A., K. Saluja, and R. Jain, "Incorporating Testability Considerations in High-Level Synthesis," *Int. Symp. Fault-Tolerant Comput.*, Boston, MA, USA, pp. 272-279, July 8-10, 1992.
- [Narayanan 92] Narayanan, S., R. Gupta, and M. Breuer, "Configuring Multiple Scan Chains for Minimum Test Time," *Int. Conf. on Comput.-Aided Des.*, Santa Clara, CA, USA, pp. 4-8, November 8-12, 1992.
- [Nozuyama 88] Nozuyama, Y., A. Nishimura, and J. Iwamura, "Design for Testability of a 32-Bit Microprocessor, the TX1," *Int. Test Conf. Proc.*, Washington, DC, USA, pp. 172-182, September 12-14, 1988.
- [Pangrle 88] Pangrle, B. M., "Splicer: A Heuristic Approach to Connectivity Binding," *25th Des. Autom. Conf.*, Anaheim, CA, pp. 536-541, June 12-15, 1988.
- [Papachristou 91] Papachristou, C. A., S. Chiu, and H. Harmanani, "A Data Path Synthesis Method for Self-Testable Designs," *28th Des. Autom. Conf.*, San Francisco, CA, USA, pp. 378-384, June 17-21, 1991.
- [Patel 93] Patel, R., and K. Yarlagadda, "Testability Features of the SuperSPARC Microprocessor," *Int. Test Conf.*, Baltimore, MD, USA, pp. 773-781, October 17-21, 1993.

- [Paulin 89a] Paulin, P. G., and J. P. Knight, "Force-Directed Scheduling for the Behavioral Synthesis of ASICs," *IEEE Trans. on Comput.-Aided Des.*, Vol. 8, No. 6, pp. 661-679, June 1989.
- [Paulin 89b] Paulin, P. G., and J. P. Knight, "Algorithms for High-Level Synthesis," *IEEE Des. and Test of Comput.*, pp. 18-31, May 1989.
- [Pilarski 92] Pilarski, S., A. Krasniewski, and T. Kameda, "Estimating Testing Effectiveness of the Circular Self-Test Path Technique," *IEEE Trans. on Comput.-Aided Des.*, Vol. 11, No. 10, pp. 1301-1316, October 1992.
- [Preissner 92] Preissner, J., G.-H. Huamann-Bollo, G. Mahlich, J. Schuck, H. Sahm, P. Weingart, D. Weinsziehr, J. Yeandel, R. Evans, "An Open Modular Test Concept for the DSP KISS-16V2," *Int. Test Conf.*, Baltimore, MD, USA, pp. 678-683, September 20-24, 1992.
- [Ratiu 90] Ratiu, I. M., and H. B. Bakoglu, "Pseudorandom Built-in Self-Test Methodology and Implementation for the IBM RISC System/6000 Processor," *IBM J. Res. Develop.*, Vol. 34, No. 1, pp. 78-84, January 1990.
- [Sentovich 92] Sentovich, E.M., J. K. Singh, C. Moon, H. Savoj, R. K. Brayton, and A. Sangiovanni-Vincentelli, "Sequential Circuit Design Using Synthesis and Optimization," *Int. Conf. on Comput. Des.*, Los Alamitos, CA, USA, pp. 328-333, 1992.
- [Sinaki 92] Sinaki, G., "C-17A Mission Computer Built-in Test and Fault Management Strategies," *IEEE National Aerospace and Electronics Conf.*, Dayton, OH, USA, pp. 822-828, May 18-22, 1992.
- [Starke 90] Starke, C. W., "Design for Testability and Diagnosis in a VLSI CMOS System/370 Processor," *IBM J. Res. Develop.*, Vol. 34, No. 2/3, pp. 355-362, March/May 1990.
- [Stroud 88] Stroud, C. E., "Automated BIST for Sequential Logic Synthesis," *IEEE Des. and Test of Comput.*, pp. 22-32, December 1988.
- [Tseng 86] Tseng, C.-J., and D. P. Siewiorek, "Automated Synthesis of Data Paths in Digital Systems," *IEEE Trans. on Comput.-Aided Des.*, Vol. CAD-5, No. 3, pp. 379-395, July 1986.
- [Turner 88] Turner, J. S., "Almost All k-Colorable Graphs Are Easy to Color," *J. of Algorithms* 9, pp. 63-82, 1988.
- [Yokomizo 92] Yokomizo, K., and K. Naito, "A 333 MHz, 72 Kb BiCMOS Pipelined Buffer Memory with Built-in Self Test," *Symp. on VLSI Circuits*, Seattle, WA, USA, pp. 32-33, June 4-6, 1992.
- [Waicukauski 89] Waicukauski, J. A., E. Lindbloom, E. B. Eichelberger, and O. P. Forlenza, "A Method for Generating Weighted Random Test Patterns," *IBM J. Res. Develop.*, Vol. 33, No. 2, pp. 149-161, March 1989.

- [Wang 86] Wang, L.-T., and E. J. McCluskey, "Concurrent Built-In Logic Block Observer (CBILBO)," *Int. Symp. on Circuits and Systems*, San Jose, CA, USA, pp. 1054-1057, May 5-7, 1986.
- [Waser 82] Waser, S., and M. Flynn, *Introduction to Arithmetic for Digital Systems Designers*, Holt, Rinehart, and Winston, 1982.
- [Zhu 88] Zhu, X.-A., and M. A. Breuer, "A Knowledge-Based System for Selecting Test Methodologies," *IEEE Des. and Test of Comput.*, pp. 41-59, October 1988.